



ifgi
Institute for Geoinformatics
University of Münster

Nighttime light images as indicators of quality of life

Master thesis

Kassiani Tsouvala

Supervisor: Prof. Dr. Edzer Pebesma

Co-Supervisor: Prof. Dr. Gilberto Câmara

March 2015

Declaration

I, Kassiani Tsouvala, declare that this thesis titled, 'Night-time light images as indicators of quality of life' and the work presented in it are my own. I confirm that:

- This work was done wholly or mainly while in candidature for a research degree at this University.
- This thesis has not been and will not be submitted in whole or in part to another University for the award of any other degree.
- Where I have consulted the published work of others, this is always clearly attributed.
- Where I have quoted from the work of others, the source is always given. With the exception of such quotations, this thesis is entirely my own work.
- I have acknowledged all main sources of help.
- Where the thesis is based on work done by myself jointly with others, I have made clear exactly what was done by others and what I have contributed myself.

Signature:

Kassiani Tsouvala

UNIVERSITY OF MUENSTER, GERMANY
Institute for Geoinformatics

KASSIANI TSOUVALA, MASTER'S OF GEOINFORMATICS

NIGHT-TIME LIGHT IMAGES AS INDICATORS OF QUALITY OF LIFE

SUMMARY

The Brazilian Amazonia has long been recognised as a repository of ecological services not only for the local communities, but also for the rest of the world. Based on information from the Brazilian Geographical and Statistics Institute IBGE¹, the region is characterised of socioeconomic inequality with an impact on human well-being.

The concept of well-being has been the concern of sciences since Aristotle (384 - 322 BC), but there is no consensus around a single definition. Different aspects to measure the human well-being include Gross Domestic Product, percentage of population with access to electric power or measuring the distribution of income in society (Ghosh et al. (2013)). In this work, we investigate a measure which is indirectly connected to well-being : electric power consumption per capita.

We explore the information provided by DMSP² satellite night-time imagery to measure the energy consumption in Brazilian Amazonia for the decade 2000 - 2010. Comparison of measured energy consumption with census data suggests it is valid to use the night-time satellite images to measure electric power consumption.

According to the World Bank³ the electricity consumption per capita is a useful unite to compare consumption between different regions. We develop an electricity consumption per capita cellular space model for the Brazilian Amazonia by developing a population distribution model and dividing with the measured electric power consumption. The model provides information with a cell resolution of 10 km.

¹<http://www.ibge.gov.br>

²<http://ngdc.noaa.gov/eog/dmsp/downloadV4composites.html>

³<http://data.worldbank.org/indicator/EG.USE.ELEC.KH.PC>

Acknowledgements

Master thesis is a compulsory part of Masters studies at Institute for Geoinformatics Muenster, Germany. First, I would like to express my gratitude towards my supervisor Prof. Dr. Edzer Pebesma⁴ for giving me the opportunity to write my thesis under his supervision. Also, I would like to thank my second supervisor Prof. Dr. Gilberto Câmara⁵ for guiding and supervising me at every step throughout the thesis period from the beginning of the research proposal.

I further thank University of Muenster for providing the opportunity to conduct this thesis work.

⁴https://www.uni-muenster.de/Geoinformatics/institute/staff/index.php/119/Edzer_Pebesma

⁵<http://www.dpi.inpe.br/gilberto>

Contents

List of Tables	vii
List of Figures	ix
1 Introduction	1
2 Methodology	3
2.1 Overview	3
2.2 DMSP night-time data	5
2.2.1 Satellites	6
2.2.2 Sensors	6
2.2.3 DMSP night-time images	7
2.3 Electric power consumption model	7
2.3.1 Geometric correction of DMSP images	7
2.3.2 Intercalibration of DMSP images	9
2.3.3 Prediction model	11
2.3.4 Intra-annual composition	14
2.3.5 Removal of gas flaring lights	14
2.3.6 Electric power consumption model	15
2.4 Population distribution model	17
2.4.1 Frequency analysis	18
2.4.2 Standardisation of values	18
2.4.3 Population disaggregation in a cell space model	20
2.5 Electric power consumption per capita model	22
3 Discussion and conclusion	24
3.1 General discussion	24
3.2 Conclusion and answer of the research question	25

3.3 Open suggestions for future research	26
Bibliography	27
A Movement schemata of geometric correction for Sicily	29
B Intercalibration scattergrams (Geometrically corrected Sicily)	33
C Testing data normality	35
D Frequency analysis and standardisation of values	38

List of Tables

2.1	Movement schemata of geometric correction for Sicily	8
2.2	Coefficients of the second order functions for each satellite for intercalibrating the annual night-time lights products	9
2.3	Comparison of intercalibration results for the State of São Paulo: Geometrically corrected Elvidge et al. (2000, 2009) method and our approach . . .	10
2.4	Percentage change of electricity consumption per state from 2000 to 2010 .	17
2.5	Values of the indicator variables are used in the quadratic functions	19

List of Figures

2.1	Brazilian Amazonia states	4
2.2	Method flowchart	5
2.3	Global DMSP-OLS Night-time Lights Time Series 1992 - 2013	6
2.4	Example showing geometric errors in DMSP images	8
2.5	Intercalibration scattergrams for the geometrically corrected night-time lights of Sicily	9
2.6	The sum of lit cell values before intercalibration for the State of São Paulo	10
2.7	The sum of lit cell values after intercalibration for the State of São Paulo .	11
2.8	Sum of lit cell values for each São Paulo municipality against public services electric power consumption	12
2.9	Sum of lit cell values for each São Paulo municipality against public services electric power consumption: (a) X axis log-transformation and (b) Y axis log-transformation	13
2.10	Sum of lit cell values for each São Paulo municipality against public services electric power consumption: X and Y axes log-transformation	13
2.11	Final prediction model: Sum of lit cell values for each São Paulo municipality against public services electric power consumption (X and Y axes log-transformation). The saturated areas are excluded (Red points)	14
2.12	Intra-annual composite for 2000 (Red circle locate the gas flare lights): (a) Corrected DMSP data (b) Corrected DMSP data excluding gas flaring	15
2.13	Measured electric power consumption (GWh) for 2000 and 2010 per Brazilian Amazonia state	15
2.14	Comparing the measured electric power consumption with census data (EPE) for 2010 per Brazilian Amazonia state	16
2.15	Comparing the measured electric power consumption with census data (EPE) for 2010 per Brazilian Amazonia state (Including gas flares)	17

2.16	Frequency analysis: (a) Distance between urban centers and (b) Electric power consumption for 2000	18
2.17	Population 2000: Comparing disaggregation model data with census data per Brazilian Amazonia state	20
2.18	Population model 2010: Comparing disaggregation model data with census data per Brazilian Amazonia state	21
2.19	Population cell model 2000 in TerraView	21
2.20	Population cell model 2010 in TerraView	22
2.21	Electric power consumption (kWh) per capita cell model 2000 in TerraView	23
2.22	Electric power consumption (kWh) per capita cell model 2010 in TerraView	23
C.1	Quantile-Quantile plot: (a) Raw Y and (b) Raw X	35
C.2	Quantile-Quantile plot: (a) Log Y and (b) Log X	35
C.3	Quantile-Quantile plot: (a) Raw X, Log Y and (b) Log X, Row Y	36
C.4	Quantile-Quantile plot: (a) Log X, Raw Y and (b) Raw X, Log Y	36
C.5	Box plot: (a) Before log-transformation (b) After log-transformation of X and Y axes	36
C.6	Residuals: (a) Against fitted values (b) Against logarithmic electric power consumption data	37
D.1	Urban nuclei distance from rivers (a) Accumulated frequency and (b) Standardized values	38
D.2	Urban nuclei distance from road network (a) Accumulated frequency and (b) Standardized values	39
D.3	Urban nuclei distance from nearest neighbour (a) Accumulated frequency and (b) Standardized values	39
D.4	Urban nuclei and forest cover 2000 (a) Accumulated frequency and (b) Standardized values	39
D.5	Urban nuclei and forest height 2010 (a) Accumulated frequency and (b) Standardized values	40
D.6	Urban nuclei distance and electric power consumption 2000 (a) Accumulated frequency and (b) Standardized values	40
D.7	Urban nuclei distance and electric power consumption 2010 (a) Accumulated frequency and (b) Standardized values	40

Chapter 1

Introduction

The *atlas of the 2010 Census*¹ by the Brazilian statistical agency (IBGE) approaches several aspects of social and regional inequalities, such as cultural and environmental diversity; demographic characteristics; urbanization; network space; socioeconomic inequalities; population structure; transport networks; and social, environmental and economic indicators. Overall, the *atlas of the 2010 Census* reflects the well-being inequality in Brazil.

Access to electric power is central to address the challenge of well-being achievement, including poverty, hunger, education, health, partnerships and environmental sustainability, as well as economic growth.

According to the World Bank Annual Report² 2013 expanding access to electricity is essential to ending poverty. The UN Millennium Project³ describes the strong links between energy services and achieving the Millennium Development Goals⁴ (MDGs). The UN Millennium Project considers that without increased investment in the energy sector, the MDGs will not be achieved in the poorest countries.

Effective policies to address the energy access problem need to be grounded in a robust information base. Night-time light images are a useful spatial indicator of electric power consumption. In this work, we explore the information provided by satellite nighttime imagery to measure energy consumption and then to estimate the well-being.

In order to better understand the change of well-being inequality, this study investigates the *electric power consumption per capita* which is indirectly connected to well-being. The area of interest is the Brazilian Amazonia region, the world's largest intact tropical rain

¹www.ibge.gov.br/english/geociencias/geografia/atlas.shtm

²<http://www.worldbank.org/annualreport2013>

³<http://www.undp.org/>

⁴<http://www.un.org/millenniumgoals>

forest of global interest, for the decade 2000 to 2010. The basis for our work is to consider previous studies in population distribution modelling and the use of nighttime lights as a population location and energy consumption indicator to develop an electric power consumption per capita model.

[Amaral et al. \(2005\)](#) analyzing the correlation between DMSP night-time light foci and electric power consumption, concluded that night-time light data are a consistent indicator of human activity and energy consumption. The analysis considering only the state of Pará in Brazil revealed a linear relation ($R^2 = 0.79$) between population of 1996 and electric power consumption ($R^2 = 0.84$) for 1999.

[Amaral et al. \(2012\)](#) propose a methodological approach to redistribute population data obtained from polygonal census tracts into population density surfaces (grids) based on a cell space database. A dasymetric map is developed using land cover data. Then, five variables are selected as indicators of human presence: distance from roads, distance from rivers, distance from urban nuclei, percentage of forest cover and slope. Fuzzy logic and hierarchical analysis procedures are applied to determine the variable weights. Finally, the census population count data are redistributed into cells. The method proposed by [Amaral et al. \(2012\)](#) was applied for the municipality of Marabá in Brazil and was subsequently adapted to the Sustainable Forest District of BR-163 municipalities.

[Briggs et al. \(2007\)](#) and [Zeng et al. \(2011\)](#) describe a GIS - based approach using remotely sensed land cover and night-time light emissions data to model population distribution at the land parcel level across the European Union. Incorporation of light emissions data was found to improve model performance considerably compared to models based only on land cover data.

The objective of this work is to answer the question raised by [Amaral et al. \(2005\)](#) paper: can we use night lights information derived from the Defense Meteorological Satellite Program⁵ (DMSP) to estimate the improvement in quality of life (well-being) through electric power consumption? For this, we investigate the spatio - temporal change of electric power consumption per capita in the Brazilian Amazonia region in the decade 2000 to 2010. We do this by developing a population distribution model and use night-time images as an indicator of electric power consumption ([Amaral et al. \(2005\)](#)).

We hypothesize that the lit areas of DMSP images represent a higher quality of life than the unlit areas. Change in night-time lights means change in the quality of life. We test this hypothesis by following the method described in Chapter 2.

⁵<http://ngdc.noaa.gov/eog/dmsp.html>

Chapter 2

Methodology

This section is structured as follows. First, we introduce the applied method by representing and describing the method flowchart (Section 2.1). Then, the DMSP night-time data are represented (Section 2.2). The steps taken to develop the electric power consumption model are described and we check the results validity comparing with census data (Section 2.2). The method of the night-time population distribution model is described and we check the reliability of the model using census data (Section 2.3). Finally, the electric power consumption per capita cell model is presented (Section 2.4) as the research result.

2.1 Overview

This study is applied to the Brazilian Amazonia (Figure 2.1) for the decade 2000 to 2010. The statistical software R¹ is used for statistical analysis of data and visualisation. In addition, the open source geographic information system, QuantumGIS² (QGIS) and python scripting language are used for data viewing, editing and processing. All of the indicator variables and data formed a TerraLib geographical database and visualised in TerraView³ GIS system taking cells as units (10km x 10km) and generating a multivalued set of cells (CellularSpace). The cellular space divided into a regular grid where each cell in the grid has one or more attributes. TerraME⁴ modelling language, an extension of the Lua programming language, is used for archival and retrieval of data stored in TerraLib geographical database. The flowchart in Figure 2.2 represents the separate steps of the research process in sequential order which are analyzed in this section.

¹www.r-project.org/

²qgis.org/en/site

³www.dpi.inpe.br/terraview_eng/index.php

⁴<http://www.terrame.org/doku.php>

Night-time light images are used to model the electric power consumption. We use sufficient cloudfree images. Ephemeral events, such as fires, sunlit data, glare, moonlit, clouds and lighting features from the aurora have been discarded. However, night light images cannot be assumed to represent a direct, linear proxy of energy consumption, but these require a suitable method of estimation before to be used.



Figure 2.1: Brazilian Amazonia states (Pa = Pará, MT = Mato Grosso, MA = Maranhao, RO = Rodonia, AM = Amazonas, TO = Tocantins, AC = Acre, AP = Amapa, RR = Roraima).

We use our approach to correct the DMSP images based on the shift - based method of satellite images geometric correctness of [Zhao et al. \(2015\)](#) and the intercalibration method developed by [Elvidge et al. \(2000, 2009\)](#). The 2.3.1 and 2.3.2 sections describe the applied method of DMSP images correctness: geometric correction, intercalibration.

[Elvidge et al. \(2000, 2009\)](#) intercalibration method uses as reference the area of Sicily, a region characterized by stable night-time lights change from 1994 to 2008. In our approach we first use the shift - based method of [Zhao et al. \(2015\)](#) to correct geometrically the area of Sicily and then apply [Elvidge et al. \(2000, 2009\)](#) intercalibration method on the global annual images.

After DMSP images correctness and since there are no electric power consumption census data for Brazilian Amazonia, the area of São Paulo is used to develop a prediction model. São Paulo is selected as an area close to the area of investigation with available census data (section 2.3.3).

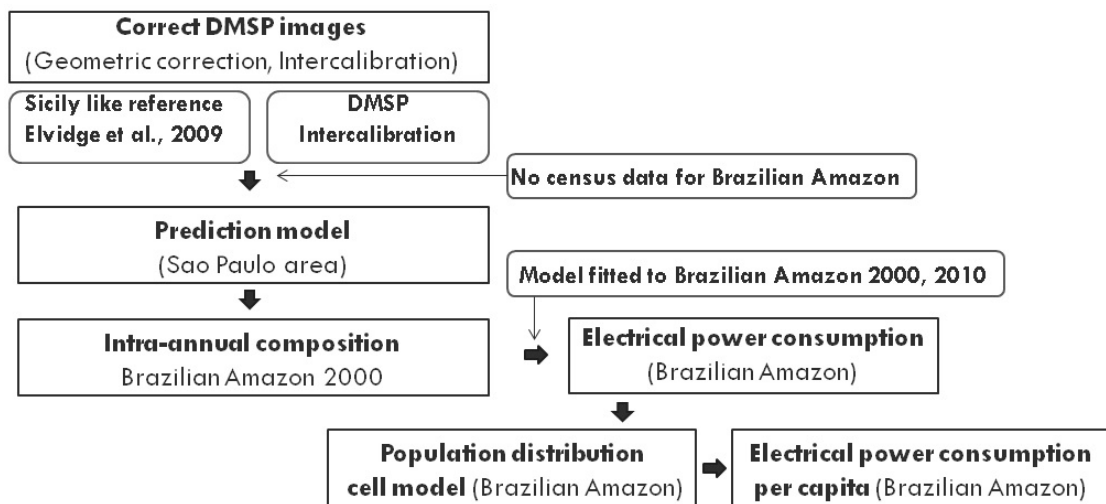


Figure 2.2: Method flowchart.

In 2000 two satellites recorded data producing two different composites (Figure 2.3: F142000, F152000). Thus, before applying the prediction model to the Brazilian Amazonia area (Section 2.3.5) and to make full use of the information derived from the two satellites, we produce one intra-annual composition applying the method Liu et al. (2012) propose (Section 2.3.4).

The section 2.4 describes the development of the population distribution cell model based on Amaral et al. (2005) method. Combining the electric power consumption and population distribution cell models, the model of electric power consumption is developed as the final step of this work.

2.2 DMSP night-time data

In the mid 1960s the Defense Meteorological Satellite Program (DMSP) of the US Department of Defense began (Doll (2008)). The DMSP, previously known as Data Acquisition and Processing Program (DAPP), was originally designed to provide visible and infrared cloud cover imagery and weather data to support Department of Defense requirements.

In 1972 the data were declassified allowing access to the civil and scientific community (Doll (2008)). However, from the time of declaration until 1992 the DMSP data were not made available by the US Department of Defense and the scientists had access to the data only from a film archive (Doll (2008)).

In 1994 the The National Geophysical Data Center (NGSC), one of three National Oceanic & Atmospheric Administration National Data Centers (NOAA, NNDC) in U.S. started working with the Defense Meteorological Satellite Program (DMSP) data. The

NGDC Earth Observation Group (EOG) specializing in nighttime data observations, uses DMSP imagery producing a time series of annual cloud free composites.

2.2.1 Satellites

The DMSP satellites fly in a sun synchronous near polar orbit at an altitude of 830 km above the surface of the earth, such that they typically pass over any area on earth between 20:30 and 21:30 local time (Elvidge et al. (2000)).

Average Visible, Stable Lights, & Cloud Free Coverages						
Year\Sat.	F10	F12	F14	F15	F16	F18
1992	F101992	-----	-----	-----	-----	-----
1993	F101993	-----	-----	-----	-----	-----
1994	F101994	F121994	-----	-----	-----	-----
1995	-----	F121995	-----	-----	-----	-----
1996	-----	F121996	-----	-----	-----	-----
1997	-----	F121997	F141997	-----	-----	-----
1998	-----	F121998	F141998	-----	-----	-----
1999	-----	F121999	F141999	-----	-----	-----
2000	-----	-----	F142000	F152000	-----	-----
2001	-----	-----	F142001	F152001	-----	-----
2002	-----	-----	F142002	F152002	-----	-----
2003	-----	-----	F142003	F152003	-----	-----
2004	-----	-----	-----	F152004	F162004	-----
2005	-----	-----	-----	F152005	F162005	-----
2006	-----	-----	-----	F152006	F162006	-----
2007	-----	-----	-----	F152007	F162007	-----
2008	-----	-----	-----	-----	F162008	-----
2009	-----	-----	-----	-----	F162009	-----
2010	-----	-----	-----	-----	-----	F182010
2011	-----	-----	-----	-----	-----	F182011
2012	-----	-----	-----	-----	-----	F182012
2013	-----	-----	-----	-----	-----	F182013

Figure 2.3: Global DMSP-OLS Night-time Lights Time Series 1992 - 2013.

Each satellite is designated with a flight number and the year (F142000 is from DMSP satellite number F14 for the year 2000). A set of annual composites is produced for each nighttime light data collection from 1992 through 2012 (Figure 2.3). Since the lifespan of a satellite is limited (6 to 8 years) and over time it is not able to record data, a replacement satellite is used to ensure continuity. Thus, in most years two satellites recorded data producing two different composites ((Elvidge et al., 2009)).

2.2.2 Sensors

The DMSP satellites use the Operational Linescan System (OLS). The OLS instrument consists of two telescopes and a photo multiplier tube (PMT). One telescope is sensitive to the visible/ near infrared radiation (0.40 - 1.10 μm) and one to the thermal/ infrared radiation (10.0 - 13.4 μm). The PMT is sensitive to radiation from 0.47 to 0.95 μm . Each

of the Operational Linescan System (OLS) of the DMSP satellites with a field of view of about 3000 km is able to provide a visible and infrared imagery of the global distribution of clouds and cloud top temperature twice per day. The images' nominal resolution is 0.56 km, which is smoothed on board into 5x5 pixel blocks to 2.8 km in order to reduce the memory usage (Doll (2008)).

2.2.3 DMSP night-time images

The DMSP OLS sensors collect global visible and infrared (IR) cloud cover data. The recorded data of each OLS sensor orbit are processed to find non-cloudy image pixels. Over a year, all the non-cloudy pixels are averaged producing a global grayscale image. The archive data set consists of low resolution global and high resolution regional of a 30 arc second grid, spanning -180 to 180 degrees longitude and -65 to 75 degrees latitude. The 30 arc-second grid spacing is equal to about 1 kilometer. That number decreases in the longitudinal direction as latitude increases. Global DMSP OLS night-time light time series from 1992 to 2012 are openly accessible from NOAA ⁵website. Two DMSP data sets are available, both made using all the available archived DMSP OLS smooth resolution data for calendar years.

The data set from NOAA under the title *Average_Lights_X_Pct* includes the night-time light product derived from the average visible band digital number (DN) of cloud free light detections multiplied by the percent frequency of light detection. This product contains detections from fires and is used to identify gas flaring volumes (Elvidge et al. (2000, 2009)).

A number of constraints are used to produce the second data set under the title *Average_Visible_Stable_Lights_and_Cloud_Free_Coverages* (Figure 2.3). Sunlit, glare, moonlit, cloud observations and aurora lighting data have been excluded producing the highest quality data for entry into the composites. This is the data set we use in this research work.

2.3 Electric power consumption model

2.3.1 Geometric correction of DMSP images

Zhao et al. (2015) discuss the geometric error in DMSP images and describes a geometric correction method. It is shown in Figure 2.4 that the correlation between F142001 and

⁵<http://ngdc.noaa.gov/eog/dmsp/downloadV4composites.html>

F162009 images is higher after shifting the second image one pixel up in vertical direction. Thus, it is necessary to execute geometric correction before the images intercalibration.



Figure 2.4: Example showing geometric errors in DMSP images. Correlation between F142001 and F162009 images is higher after shifting F162009 one pixel up in vertical direction

We use the F142001 image as a reference image since it was arbitrarily selected by [Zhao et al. \(2015\)](#) to perform the geometric correction for Sicily. We shift each annual image with 25 different movement combinations (horizontally: left or right, vertically: up or down) and we calculate the correlation coefficient of DN values between the shifted and the reference image. The shift gives the highest correlation coefficient when the geographic positions of the two images are the closest. Table 2.1 exhibits the best movement schemata of the geometric correction for Sicily (See Appendix A).

Satellite	Movement scheme	Original correlation	Largest correlation
F121999	Left 1pixel	0.9698	0.9732
F141999	None	0.9832	0.9832
F142000	None	0.9855	0.9855
F142001	None	1.0000	1.0000
F142002	None	0.9691	0.9691
F142003	None	0.9825	0.9825
F152000	Left 1pixel - Up 1pixel	0.9585	0.9726
F152001	Left 1pixel	0.9716	0.9796
F152002	Left 1pixel	0.9765	0.9806
F152003	None	0.9671	0.9671
F152004	None	0.9775	0.9775
F152005	Left 1pixel	0.9604	0.9699
F152006	None	0.9764	0.9764
F152007	None	0.9761	0.9761
F162004	Up 1 pixel	0.9532	0.9643
F162005	None	0.9789	0.9789
F162006	None	0.9762	0.9762
F162007	None	0.9725	0.9725
F162008	Left 1pixel	0.9628	0.9697
F162009	Up 1 pixel	0.8922	0.9568
F182010	Up 1 pixel	0.9026	0.9563

Table 2.1: Movement schemata of geometric correction for Sicily.

2.3.2 Intercalibration of DMSP images

Because the OLS has no on-board calibration; thus, digital number (DN) values are incompatible across different years. [Elvidge et al. \(2000, 2009\)](#) propose an empirical procedure of intercalibration that we apply in the DMSP data set from 1999 to 2010.

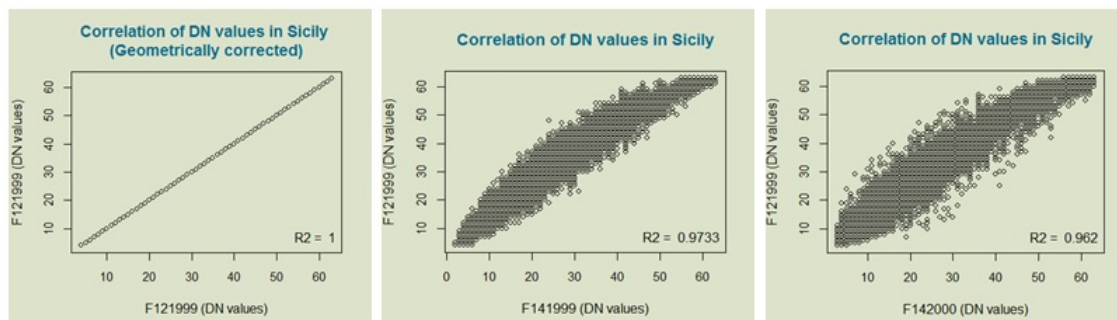


Figure 2.5: Intercalibration scattergrams for the geometrically corrected night-time lights of Sicily.

The F121999 image for Sicily is used as a reference image because it has the largest range of DN values, a valuable characteristic since it permits a higher accuracy of the second - order functions [Zhao et al. \(2015\)](#).

$DN_{adjusted} = C_0 + C_1 \times DN + C_2 \times DN^2$			
Satellite	C0	C1	C2
F121999	0	1	0
F141999	-0.1609	1.51	-0.008028
F142000	1.23	1.311	-0.00523
F142001	0.3652	1.315	-0.00509
F142002	1.1904703	1.1588843	-0.003075
F142003	0.838	1.246	-0.004036
F152000	0.1786	1.04	-0.0009323
F152001	-0.7237	1.122	-0.001538
F152002	0.1224818	0.9698998	0.0008204
F152003	0.3407405	1.5028275	-0.0078444
F152004	0.7005	1.324	-0.005058
F152005	0.7479	1.268	-0.004032
F152006	0.8868	1.276	-0.00414
F152007	1.5991162	1.2592894	-0.0039692
F162004	0.3260005	1.184088	-0.0032429
F162005	0.1714	1.393	-0.006027
F162006	0.1073501	1.1450422	-0.001861
F162007	0.8857	0.886	0.001601
F162008	0.6499	0.9824	0.0000536
F162009	0.9343773	1.0665173	-0.0015392
F182010	1.907883	0.51871	0.006848

Table 2.2: Coefficients of the second order functions for each satellite for intercalibrating the annual night-time lights products.

We develop a group of second order regression functions by adjusting DN values of

pixels in Sicily of candidate respective images to the match DN values of pixels in Sicily in the reference image. Figure 2.5 shows examples of the scattergrams for each year of the satellite images of Sicily versus F121999 (See Appendix B).

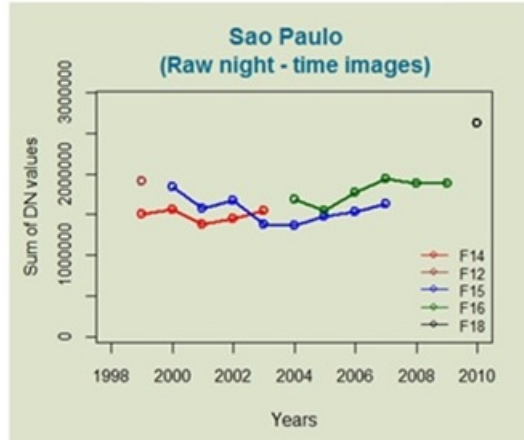


Figure 2.6: The sum of lit cell values before intercalibration for the State of São Paulo.

Then, we apply these functions to the corresponding satellite images to build intercalibrated DMSP images. The coefficients of the second order functions for each satellite is shown in Table 2.2.

The objective of the intercalibration is to have continuity of the sum of the lights index values from each year of the time series. One sign of a successful intercalibration is the convergence of values in years where two satellite products are available (Elvidge et al. (2000, 2009)).

After intercalibration, pixels with original DN value of zero have nonzero values. To achieve reliable pixel values, a threshold value is used. Since there is no pixel with DN value smaller than 3, we use this value as a threshold value assuming that DN values smaller or equal to 3 have DN value of zero in intercalibrated images.

State of Sao Paulo				
Satellites			Absolute values	
	Elvidge & Geom. Correction	Our approach	Elvidge & Geom. Correction	Our approach
F141999 - F121999	-23303.01	-26402.01	23303.01	26402.01
F152000 - F142000	-41591.11	-32662.07	41591.11	32662.07
F152001 - F142001	-18008.1	-14938.05	18008.10	14938.05
F152002 - F142002	-3314302.11	-3326188.57	3314302.11	3326188.57
F152003 - F142003	-13646.15	-8130.72	13646.15	8130.72
F162004 - F152004	201324.57	204349.19	201324.57	204349.19
F162005 - F152005	133935.74	120296.09	133935.74	120296.09
F162006 - F152006	-84539.25	-78731.77	84539.25	78731.77
F162007 - F152007	-110745.08	-115032.67	110745.08	115032.67

Table 2.3: Comparison of intercalibration results for the State of São Paulo: Geometrically corrected Elvidge et al. (2000, 2009) method and our approach.

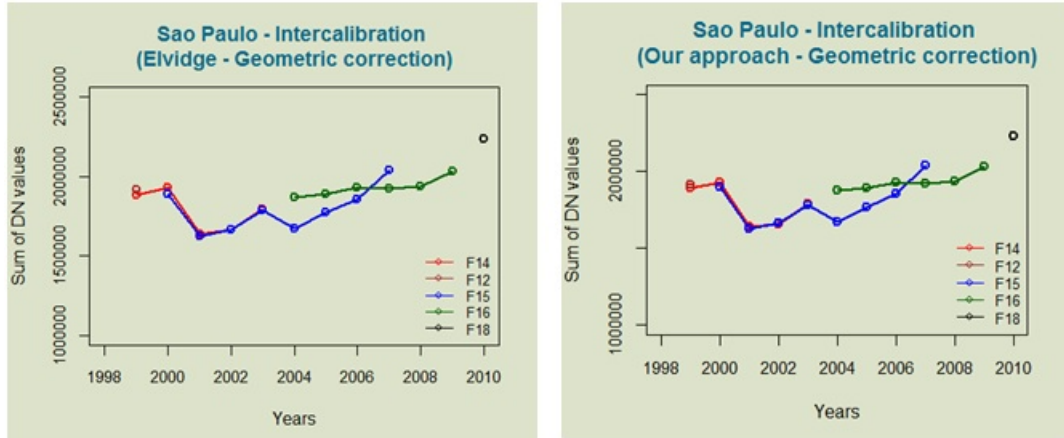


Figure 2.7: The sum of lit cell values after intercalibration for the State of São Paulo: (a) Geometrically corrected Elvidge et al. (2000, 2009) method, (b) Our approach.

The graphs in figures 2.5 and 2.6 display the sum of lit cell values before and after intercalibration respectively for the state of São Paulo. Table 2.3 compares the results of the geometrically corrected Elvidge et al. (2000, 2009) intercalibration method and our approach, concluding that our approach gives better results for the DMSP images of 2000 (F142000, F152000). Thus, we use the intercalibrated images produced from our approach for the rest of the research method.

2.3.3 Prediction model

We build the prediction model using electricity consumption census data from the site of the Foundation State System Data Analysis⁶ agency (SEADE).

SEADE is an agency of the Department of Planning and Regional Development of the Government of the state of São Paulo providing free access to electricity consumption data sets. The data sets are classified according to consumer type in public services, industrial, residential, rural and commercial electricity consumption per municipality.

Before building the prediction model we take a first look at the data for checking the relation between the DMSP night-time lights and each of the electric power consumption category (Figure 2.8).

Plotting the sum of lit cell values for each São Paulo municipality against each electricity consumption census category and applying a linear model, we observe that the category of public services electric power consumption gives the highest correlation ($Cor = 0.74$) and coefficient of determination ($R^2 = 0.55$) with the sum of DMSP cell values (Figure

⁶<http://www.seade.gov.br/>

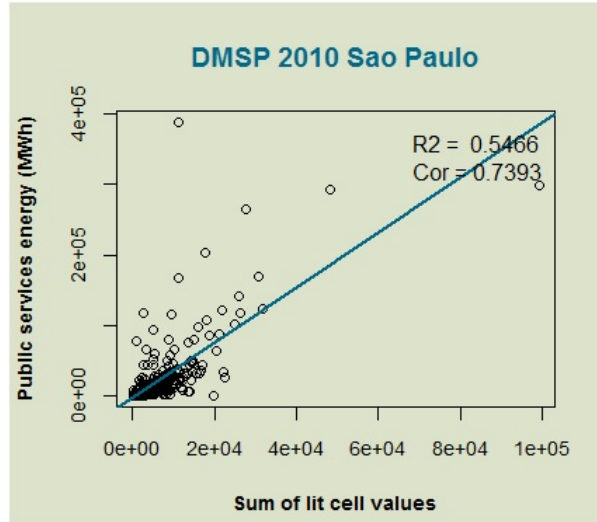


Figure 2.8: Sum of lit cell values for each São Paulo municipality against public services electric power consumption.

2.8). This can be explained by the satellite recording of public outdoor lights emissions (Exterior lighting of streets and buildings) and not indoor lighting.

Observing the cone-shaped plot in Figure 2.8, we assume heteroscedasticity. In statistics, heteroscedasticity is the absence of homoscedasticity and this means the variability of a variable (Sum of lit cell values) is unequal across the range of values of a second variable that predicts it (Public services electric power consumption).

We test the heteroscedasticity assumption applying the classical Levene's test. Levene's test evaluates the equality of variances for a variable measured for two or more groups. It tests the null hypothesis that variances of different samples from the same population are equal. If the P-value of Levene's test is less than 0.05 the null hypothesis of equality is rejected. The resulted P - value for our data is less than 0.05 and equal to $3.263e^{-6}$, concluding that there is a difference between the variances and the data are heteroscedastic.

There are several approaches to deal with heteroscedasticity and the logarithmic transformation is the most common one. We apply the logarithmic transformation in X and Y axis separately (Figure 2.9) and together (Figure 2.10). The both axis log-transformation returns the best results with data distribution closest to the normal (Figure 2.10).

The assumption of normality is checked with the graphical methods of quantile-quantile plot (Q-Q plot), box-plot, residuals plot and skewness measurement before (Skewness(X) = 7.49, skewness(Y) = 6.57) and after (Skewness(X) = 0.11, skewness(Y) = 0.68) log-transformation (See Appendix C). The plot in Figure 2.10 represents the data distribution after the log-transformation and the applied exponential model ($R^2 = 0.72$).

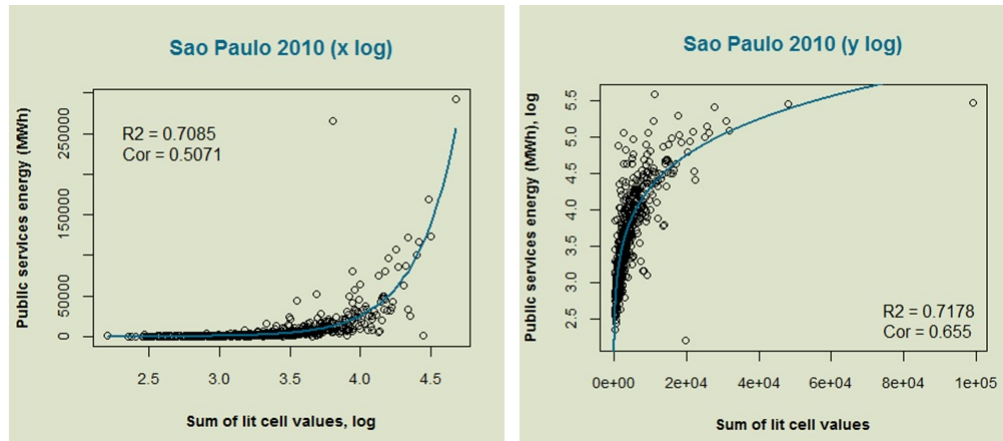


Figure 2.9: Sum of lit cell values for each São Paulo municipality against public services electric power consumption: (a) X axis log-transformation and (b) Y axis log-transformation.

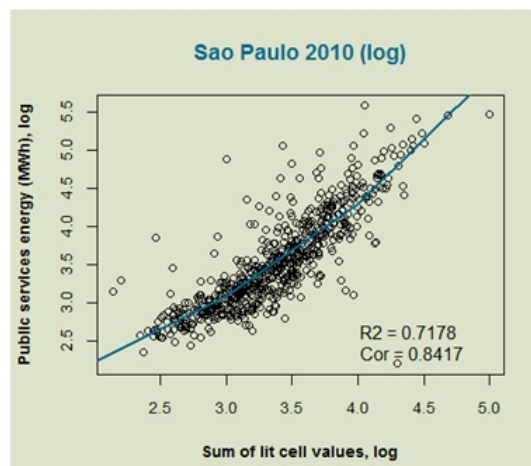


Figure 2.10: Sum of lit cell values for each São Paulo municipality against public services electric power consumption: X and Y axes log-transformation.

To improve more the prediction model, the metropolitan area (São Paulo) and the states on border with it discarded from the data set (Greater São Paulo). These areas are affected from the saturation effect and considered as outliers because of overestimation of lit cell values (Amaral et al. (2005)). After discarding the outliers, 602 states left in the data set out of the total number of 638 states. In Figure 2.11 the red points of the plot are the excluded values (Outlier states). The exponential model in Figure 2.11 ($R^2 = 0.79$) is improved from the model in Figure 2.10 ($R^2 = 0.72$) and this is the final prediction model we use for the rest of this work ($y = 1.1406 e^{0.329x}$).

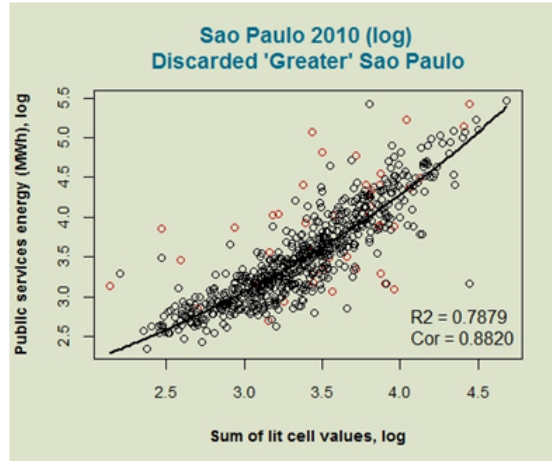


Figure 2.11: Final prediction model: Sum of lit cell values for each São Paulo municipality against public services electric power consumption (X and Y axes log-transformation). The saturated areas are excluded (Red points).

2.3.4 Intra-annual composition

The objective of intra-annual composition is to make full use of the information derived from the two satellites F142000 and F152000. To do this, we based our approach on the method proposed by Liu et al. (2012). Lit pixels detected by only one satellite are defined as unstable lit pixels and replaced with zero value. Stable lit pixels are replaced by the average DN value of them. In this way, one intra-annual composite is produced for 2000 for the Brazilian Amazonia.

$$DN(2000, i) = \begin{cases} 0 & DN_{(2000,i)}^{F14} = 0 | DN_{(2000,i)}^{F15} = 0 \\ (DN_{(2000,i)}^{F14} + DN_{(2000,i)}^{F15})/2 & \text{otherwise} \end{cases} \quad (2.1)$$

Where $DN_{(2000,i)}^{F14}$ and $DN_{(2000,i)}^{F15}$ are DN values of the same i th lit pixel from the two satellite images F14 and F15 of 2000.

2.3.5 Removal of gas flaring lights

We define the cells lighting because of gas flaring overlapping the Brazil Gas Flaring Shapefile from NOAA⁷ site. We set the values of these cells equal to the zero value since these represent neither electric power consumption nor inhabitant areas (Figure 2.12).

⁷http://ngdc.noaa.gov/eog/interest/gas_flares_countries_shapefiles.html

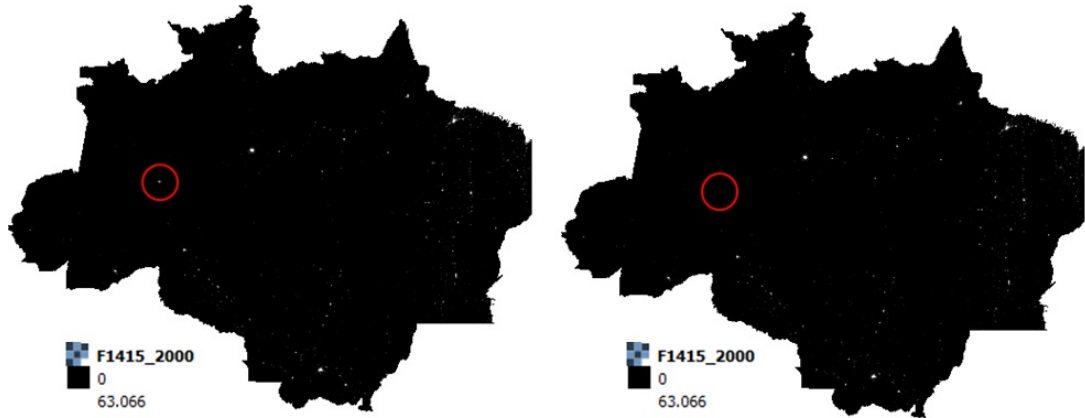


Figure 2.12: Intra-annual composite for 2000 (Red circle locate the gas flaring): (a) Corrected DMSP data (b) Corrected DMSP data excluding gas flaring.

2.3.6 Electric power consumption model

We apply the developed exponential prediction model (Figure 2.11) to the calibrated and gas flaring clean DMSP images F182010 and F14,152000 (Intra-annual composition: 2.3.4 section) of the Brazilian Amazonia area. Then, we transform the predicted DN values to non logarithmic scale and measure the electric power consumption for 2000 and 2010 in every state of the Brazilian Amazonia summing the cell values (Figure 2.13).

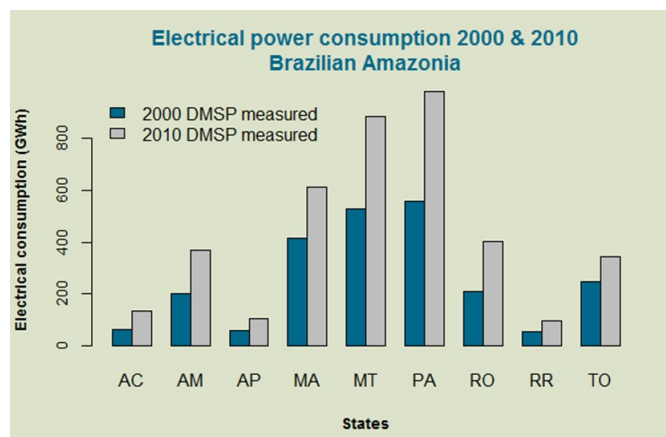


Figure 2.13: Measured electric power consumption (GWh) for 2000 and 2010 per Brazilian Amazonia state (Pa = Pará, MT = Mato Grosso, MA = Maranhao, RO = Rondonia, AM = Amazonas, TO = Tocantins, AC = Acre, AP = Amapa, RR = Roraima).

Census data obtained from the Brazilian Government's Energy Research Agency⁸ (EPE) validate the measured results (Figure 2.14). As mentioned in the 2.3.3 section, the satellite records represent the public outdoor lights emissions (Exterior lighting of

⁸<http://www.epe.gov.br/>

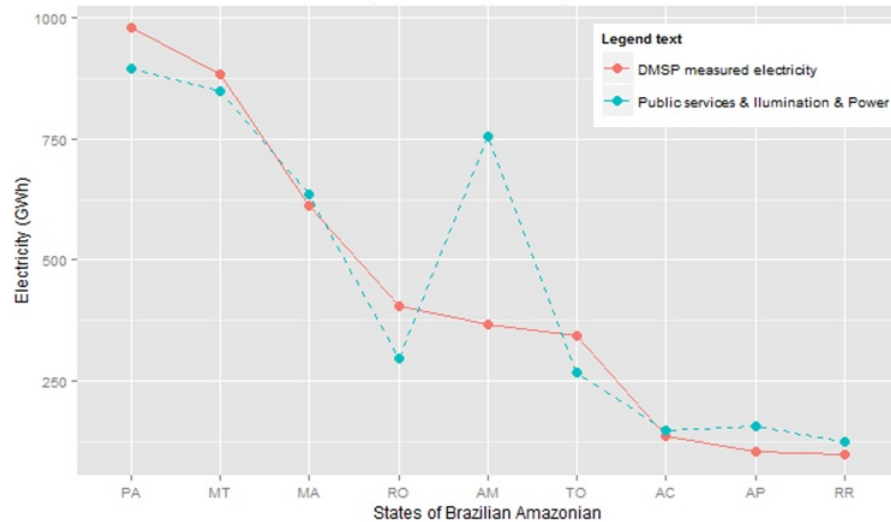


Figure 2.14: Comparing the measured electric power consumption with the census data (EPE) for 2010 per Brazilian Amazonia (Pa = Pará, MT = Mato Grosso, MA = Maranhao, RO = Rondonia, AM = Amazonas, TO = Tocantins, AC = Acre, AP = Amapa, RR = Roraima).

streets and buildings) and not indoor lighting. Thus, we compare the sum of the public electricity consumption census data categories as these are classified in the EPE annual report ⁹ 2010: public services, public illuminationn, public power electric power consumption.

At a first glance, there is a difference between the measured results and the census data. Especially for the Amazonas state where the difference is big. Although the data are not overlapped, the measured results are valid since there is no direct interpretation between satellite records and census data records. No direct interpretation means that part of other electric power consumption categories (Residential, industrial, commercial and rural) may be included in our results as an extension of the DMSP satellite records. For instance, outdoor lights of yards, shops and industries is possible to be included in the DMSP night-time light records.

Regarding the big difference between the measured result and census data of the Amazonas state, we refer that this is the area where we set the gas flaring lit cell values equal to the zero value. One thought was that the gas flaring light is included into the electrical power consumption census records. However, including the gas flaring lit cells in our measurement does not improve enough the measured electricity consumption (Figure 2.15). The state of Amazonas is considered as an outlier. We discuss this in *Open*

⁹www.epe.gov.br/AnuarioEstatisticodeEnergiaEletrica/20130909_1.pdf

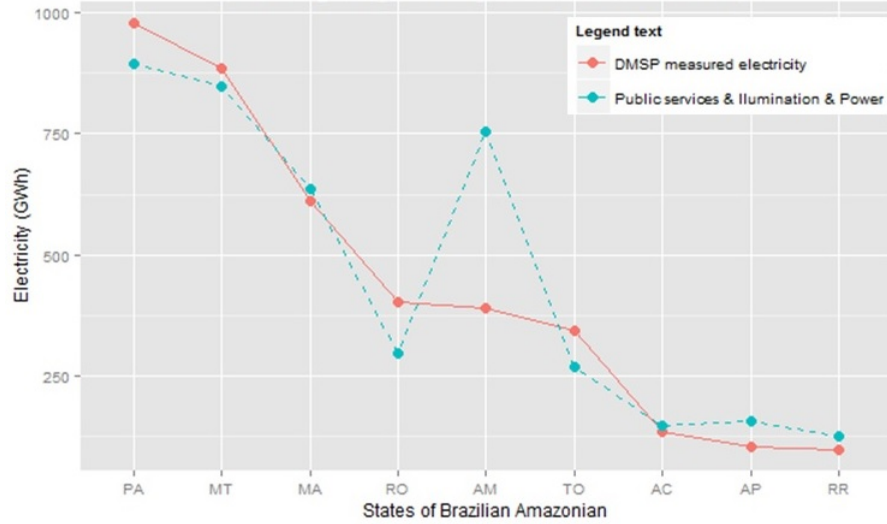


Figure 2.15: Comparing the measured electric power consumption with the census data (EPE) for 2010 per Brazilian Amazonia state, including gas flares (Pa = Pará, MT = Mato Grosso, MA = Maranhao, RO = Rondonia, AM = Amazonas, TO = Tocantins, AC = Acre, AP = Amapa, RR = Roraima).

State (Full name)	State	Electricity consumption 2000 (GWh)	Electricity consumption 2010 (GWh)	Change in electricity consumption % (2000 - 2010)
Acre	AC	65.10	135.76	109%
Amazonas	AM	203.37	367.52	81%
Amapa	AP	57.62	104.54	81%
Maranhao	MA	416.38	612.62	47%
Mato Grosso	MT	526.64	885.63	68%
Para	PA	556.82	979.69	76%
Rondonia	RO	208.25	403.66	94%
Roraima	RR	56.45	97.03	72%
Tocantins	TO	248.36	343.39	38%

Table 2.4: Percentage change of electricity consumption per state from 2000 to 2010.

suggestions for future research section (Section 3.3).

To explore more the results, we calculate the percentage change of electricity consumption per state from 2000 to 2010 (Table 2.4). The electric power consumption is increasing in every state. The states of Acre (109%) and Rondonia (94%) have the largest increase and state of Tocantins (38%) the lowest.

2.4 Population distribution model

Population estimation methods can be grouped into two categories: areal interpolation and statistical modelling. Areal interpolation methods can be further separated into two categories depending on whether ancillary information is used (Wu et al. (2005)).

We based on the population distribution method proposed by [Amaral et al. \(2012\)](#) to generate a cellspace (10km x 10km) model of night time urban population distribution.

We investigated the usage of five variables: distance from roads, distance from rivers, distance from urban nuclei (nearest neighbor distance), percentage of forest cover for 2000, forest height for 2010 and electric power consumption data (Measured from DMSP night-time images, section 2.3).

2.4.1 Frequency analysis

Location of urban nuclei is assumed to be evidence of human presence [Amaral et al. \(2012\)](#). Thus, we first identify the relationship between each indicator variable and the location of urban nuclei. Each variable is studied individually applying a frequency analysis (See Appendix D). From the frequency analysis of distance between urban centers, it is observed that 90% of the communities are less than or equal to 25.1 km away from the nearest neighbor (Figure 2.16(a)). Regarding the electric power consumption for 2000, 50% of the communities consume less or equal to 10 MWh and 90% consume less than or equal to 43 MWh (Figure 2.16(b)).

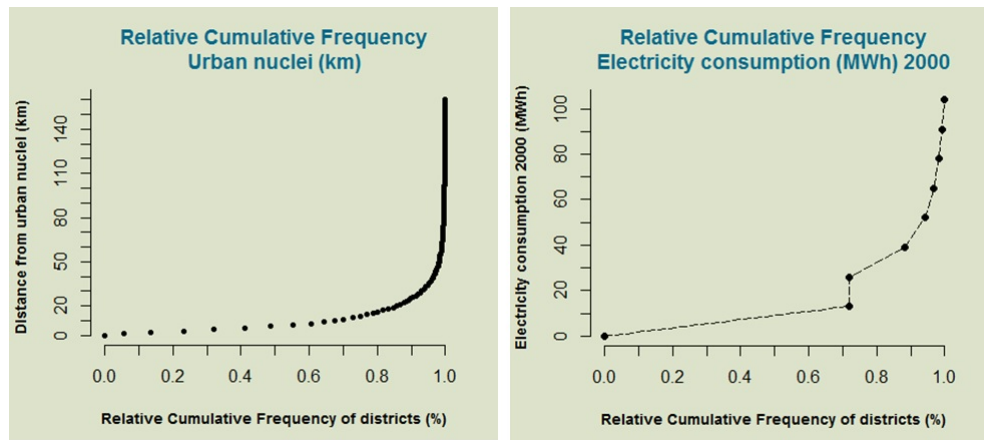


Figure 2.16: Frequency analysis: (a) Distance between urban centers and (b) Electric power consumption for 2000.

2.4.2 Standardisation of values

The scale and range of each indicator variable is different. Thus, before start the operations between the variables, there is a need for standardisation of values. We standardize the values applying the quadratic functions [Amaral et al. \(2012\)](#) describe.

Taking the distance between urban centers (z) as an example, the quadratic functions are as follows:

$$F(x) = \begin{cases} 0 & \text{if } z \leq 160.59 \text{ km} \\ 1/(1 + a(z - b)^2) & \\ 1 & \text{if } z \geq 160.59 \text{ km} \end{cases} \quad (2.2)$$

The b value corresponds to the value of the variable when the possibility of having associated population is maximum. The value of alpha (a) corresponds to the value of the variable where the occurrence or non-occurrence of the population is equal (50%) and is calculated by the equation:

$$a = \frac{1}{(z - b)^2} \quad (2.3)$$

Where z is the value of the variable when $F(z) = 0.5$. Table 2.5 shows the values of the indicator variables that are used in the quadratic functions.

Indicator variable	z	$f(z)$	α	β
Distance to roads (km)				
\leq	0.9	1		
$=$	4	0.5	0.1046	0.9
$>$	164.46	0		
Distance to river (km)				
\leq	0.9	1		
$=$	26	0.5	0.00172	0.9
$>$	260.43	0		
Distance to urban nuclei (km)				
\leq	1	1		
$=$	6.2	0.5	0.03698	1
$>$	160.59	0		
Forest cover 2000 (%)				
\leq	1	1		
$=$	76	0.5	0.000178	1
$>$	100	0		
Forest height 2010 (m)				
\leq	0	1		
$=$	13.5	0.5	0.0059172	0
$>$	40	0		
Electricity 2000 (MWh)				
\geq	114	1		
$=$	10	0.5	9.246E-05	114
$<$	1	0		
Electricity 2010 (MWh)				
\geq	118	1		
$=$	11	0.5	8.734E-05	118
$<$	1	0		
Electricity 2000 (MWh) - Urban				
\geq	112	1		
$=$	41	0.5	0.0001984	112
$<$	1	0		
Electricity 2010 (MWh) - Urban				
\geq	112	1		
$=$	46	0.5	0.0002261	112
$<$	1	0		

Table 2.5: Values of the indicator variables are used in the quadratic functions.

2.4.3 Population disaggregation in a cell space model

In this section, we discuss the disaggregation of the urban population census data (Source: IBGE) in a cell space with 10 km cell resolution (Urban population 2000 = 14.366.161 and urban population 2010 = 18.299.227). To disaggregate population from census data to the cell space we based on the method proposed by [Amaral et al. \(2012\)](#), but we changed the used disaggregation equation. Applying the disaggregate equation proposed by [Amaral et al. \(2012\)](#) in our area and data, it does not work properly.

According to the probability theory we find the probability of dependent events by multiplying the probabilities of each previous event. Disaggregating population in a cell space using multiple indicators per cell, the population presence probability of one cell is affected by all of the indicators. Applying the disaggregation equation (2.4) and considering indicators as dependent variables, in our research the F_{grid_i} value resulted from the multiply of $F(z)$ indicator variables and not from the weight average as [Amaral et al. \(2012\)](#) describe. P_{grid_i} is the population count to be attributed to a grid cell (i), P_{CT_I} is the total urban population, F_{grid_I} is the sum of all F_{grid_i} and i is a grid cell of the cell space I .

$$P_{grid_i} = P_{CT_I} * \frac{F_{grid_i}}{F_{grid_I}} \quad (2.4)$$

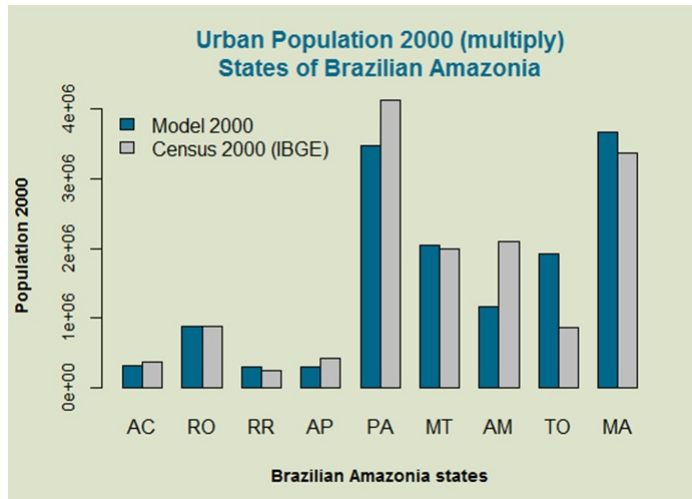


Figure 2.17: Population 2000: Comparing disaggregation model data with census data per Brazilian Amazonia state (Pa = Pará, MT = Mato Grosso, MA = Maranhao, RO = Rodonia, AM = Amazonas, TO = Tocantins, AC = Acre, AP = Amapa, RR = Roraima).

Importing the indicator variables in TerraView GIS system and using the plug-in *Fill cell*, each cell is filled with one value for each indicator variable. We process the data

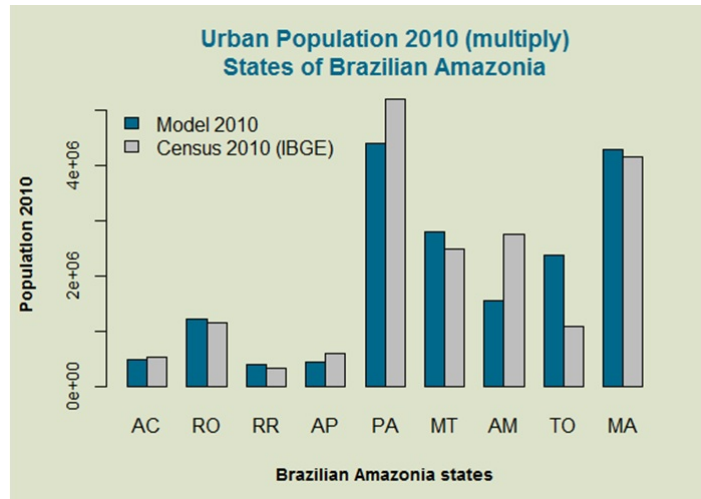


Figure 2.18: Population model 2010: Comparing disaggregation model data with census data per Brazilian Amazonia state (Pa = Pará, MT = Mato Grosso, MA = Maranhao, RO = Rondonia, AM = Amazonas, TO = Tocantins, AC = Acre, AP = Amapa, RR = Roraima).

using the Lua programming language and test different combinations of indicators to disaggregate the urban population into the cell space.

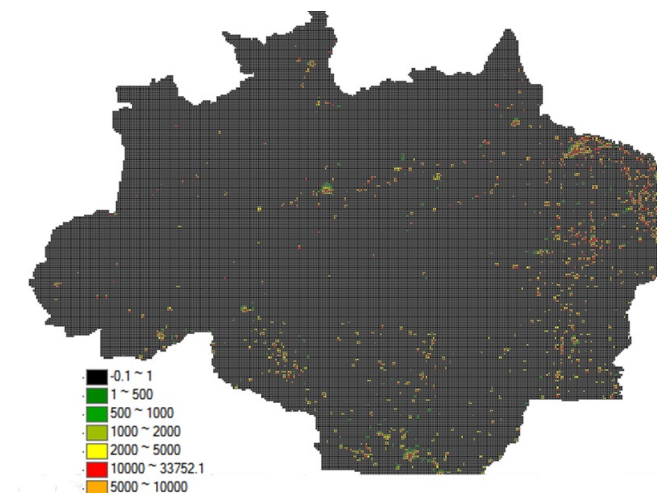


Figure 2.19: Population cell model 2000 in TerraView.

Also, we tested the approach of excluding cells characterised as river area (Ancillary information) considering that population presence is not occurring in water areas. Each combination disaggregation is validated by measuring the disaggregated population in every state and comparing with census data respectively. DMSP satellites are capable to record urban centers with population higher than 400.000 inhabitants (Amaral et al. (2012)). Thus, we disaggregate the urban and not the total population which probably

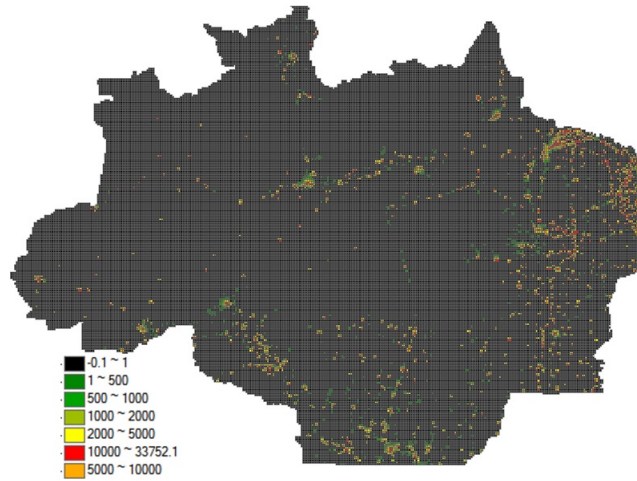


Figure 2.20: Population cell model 2010 in TerraView.

includes number of people inhabit in villages and other smaller areas.

The two variables of electric power consumption and distance from urban nuclei (nearest neighbor distance) return the best tested population disaggregation result (Figures 2.17, 2.18). The water areas are included to the final model. The resolution is low (10km x 10km) and excluding the water area cells we possibly lose a big part of the populated area.

The two column plots in Figures 2.17 and 2.18 compare the model result with census data. Observing the plots, the model does not work well for the two states of Tocantins and Amazonas, but it returns good results for seven out of nine states. This is the best achieved model and is the one we use to develop the electric power consumption per capita model in section 2.5.

After applying the disaggregation method as it is described in the previous section the two population distribution models for 2000 and 2010 are developed and visualized in TerraView GIS system with a cell space resolution 10 km (Figures 2.19, 2.20).

Observing the two population models we take a general view of the population change and point out the places with less or more change from 2000 to 2010. Population tends to gather at the district seats with a higher concentration towards big city centers.

2.5 Electric power consumption per capita model

After the development of the population model, each cell of the cell space includes values of electrical power consumption and population for 2000 and 2010.

We develop two electric power consumption per capita cell space models for 2000 and 2010 respectively. In the same way as in population developing model, we use the Lua

script language to process the cell values. Dividing the electric power consumption value with the population value of each cell we fill each cell with the new value of the electrical power consumption per capita.

Two models are generated for 2000 and 2010 respectively with the same cell resolution (10 km) as the population distribution model. The two models are visualised in Figures 2.21, 2.22. As it was expected cells with zero electrical power consumption value have also zero electrical power consumption per capita (Figures 2.21, 2.22: Black area).

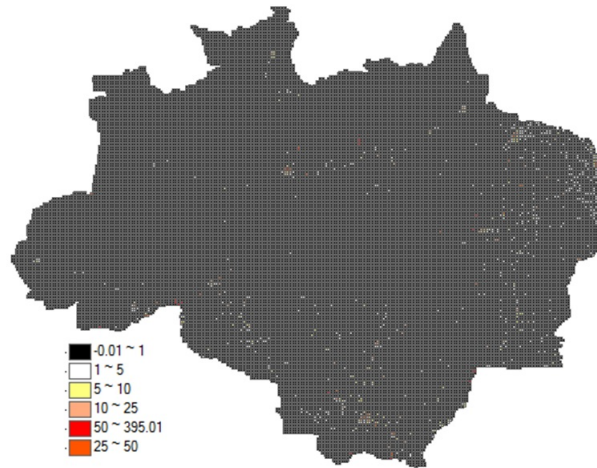


Figure 2.21: Electric power consumption (kWh) per capita cell model 2000 in TerraView.

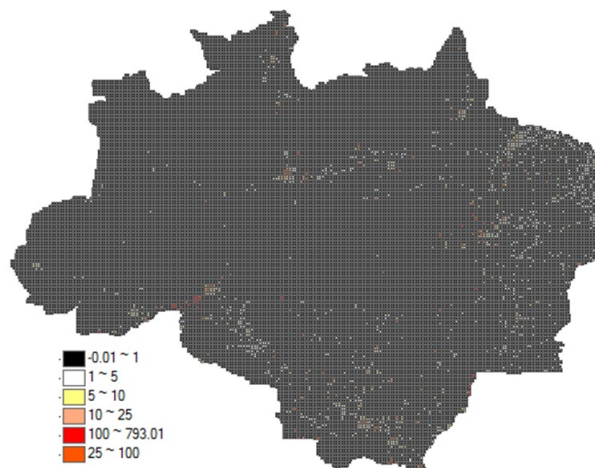


Figure 2.22: Electric power consumption (kWh) per capita cell model 2010 in TerraView.

Chapter 3

Discussion and conclusion

3.1 General discussion

In this section, we point out and discuss the most important parts of the applied research method and relate these with previous works.

The usage of clean and intercalibrated DMSP images is an important part of this research. The raw DMSP images from NOAA site are already cleaned from ephemeral lights, but gas flaring lights should also be removed. Also, the intercalibration of the satellite images is a crucial step. [Elvidge et al. \(2000, 2009\)](#) in previous researches describe an intercalibration method of DMSP images. [Zhao et al. \(2015\)](#) in a new research paper expand [Elvidge et al. \(2000, 2009\)](#) method mentioning and suggesting the geometrical correction of DMSP images. In this research, the geometric correction takes first place and then the intercalibration method of [Elvidge et al. \(2000, 2009\)](#). This gives better result for the satellite images of our interest F142000 and F152000 (Figure 2.7).

[Amaral et al. \(2005\)](#) investigating the state of Pará, conclude that there is a linear relation between DMSP and electric power consumption. We improve [Amaral et al. \(2005\)](#) model for the state of São Paulo (Figure 2.8) by dealing with the heteroscedastic distribution of the data. An exponential model is developed (Figure 2.11) and applied to the Brazilian Amazonia area to develop an electric power consumption prediction model.

[Amaral et al. \(2012\)](#) develop a population distribution method for the municipality of Marabà and apply this to the Sustainable Forest District of BR-163 municipalities of Brazil. Adapting this method to the Brazilian Amazonia area the model does not work properly for the Brazilian Amazonia, a bigger area with different natural and social characteristics. Following the [Amaral et al. \(2012\)](#) method, but changing the disaggregation equation based on the probability theory for dependent events and using just the two

indicator variables of electric power consumption and distance from urban nuclei, the population model works properly for the seven out of nine states.

3.2 Conclusion and answer of the research question

The study is applied to the Brazilian Amazonia for the decade 2000 to 2010 and research whether the information deriving from the Defence Meteorological Satellite Program (DMSP) can be used to estimate the improvement in quality of life through electric power consumption.

The resulted plot in Figure 2.14 represents that the electricity values measured using DMSP images are close to the census data. This plot gives positive answer to the research question. The applied method suggests it is possible to use the DMSP nighttime lights to measure the public electric power consumption.

However, as it is referred in section 2.3.6, since there is not direct interpretation between satellite records and census data records, outliers may occur like the state of Amazonas in our research area.

As it is referred in the beginning of this work access to electricity is related to the issue of well-being. Lack of or low access to modern energy services drives to energy poverty and electric power consumption per capita is an indicator for measuring this. According to the World Bank¹ the richest country in electric power consumption is Iceland in 2000 (26.202 kWh per capita) and 2010 (51.440 kWh per capita). The poorest in electricity are Ethiopia in 2000 (23 kWh per capita) and Haiti in 2010 (25 kWh per capita).

Comparing the developed models of electric power consumption per capita for 2000 and 2010 we get the information that in general the electrical consumption per capita is increasing in this decade. The cell values of the two models (2000 and 2010) are easily accessible through TerraView interface making it easy to compare smaller areas up to 100 km^2 (10km x 10km). Also, cell space models offer advantages over areal unit representation (Coropleth mapping) (Mennis (2003)). Cell models can have higher resolution and are not affected from geopolitical boundary changes.

The cell values can be extracted and stored as a csv or shapefile format for further calculations or processed with Lua script language. Analysing further these data we can point out the poorest and richest in electricity per capita areas and areas with or without increase in the decade 2000 to 2010. In this way we have a higher resolution of the problem and our intervention will be more effective.

¹<http://www.worldbank.org/>

3.3 Open suggestions for future research

As it is referred in the previous section the state of Amazonas is an outlier (Figure 2.14). The capital city of Manaus, the most populous city in the Brazilian Amazonia, may be affected by the saturation effect with an impact to the results. Manaus is in the state of Amazonas and we could try excluding the census electricity data from this area.

Overall, it is possible to improve the results precision by cleaning the DMSP nighttime light images from the saturation and blooming effect. Blooming is caused due to surface reflection and saturation due to the accumulated light of big city centers. The effect of blooming may overestimate the spatial extent of electric power consumption and the effect of saturation overestimate the DN cell value. A low light threshold of detection frequency can be used to reduce the overestimated spatial extent of light area. However, applying a single threshold attenuates large numbers of smaller lights and significantly reduces the information content of the night lights data sets (Small et al. (2005)). For this reason no single brightness threshold is valid for all light images (Ma et al. (2012)).

The electrical power consumption per capita cell model can also be improved using the dasymetric method. The dasymetric method is an areal interpolation method which uses available ancillary data to provide further insight into the probable population distribution. The dasymetric method commonly regarded as the most accurate approach of all population estimation methods (Wu et al. (2005)). The waterlands (e.g., lakes, rivers) can be identified waterlands (e.g., lakes, rivers) using land cover data and characterise these as unpopulated areas (Amaral et al. (2012)).

Before using the dasymetric method we should take under consideration the cell space resolution of the model. The cell resolution should be less than 10 km (Current research method resolution) since a coarse resolution excludes inhabited areas and affects the population distribution model. The resolution can be improved to 1 km (Resolution of DMSP satellite images) using an upgraded hardware system.

Bibliography

- Amaral, S., Câmara, G., Monteiro, A. M. V., Quintanilha, J. A., and Elvidge, C. D. ((2005)). Estimating population and energy consumption in Brazilian Amazonia using DMSp night-time satellite data. *Computers, Environment and Urban Systems*, 29(2):179–195. [2](#), [5](#), [13](#), [24](#)
- Amaral, S., Gavlak, A. A., Escada, M. I. S., and Monteiro, A. M. V. ((2012)). Using remote sensing and census tract data to improve representation of population spatial distribution: case studies in the Brazilian Amazon. *Population and Environment*, 34(1):142–170. [2](#), [18](#), [20](#), [21](#), [24](#), [26](#)
- Briggs, D. J., Gulliver, J., Fecht, D., and Vienneau, D. M. ((2007)). Dasymetric modelling of small-area population distribution using land cover and light emissions data. *Remote Sensing of Environment*, 108(4):451–466. [2](#)
- Doll, C. N. H. (2008). CIESIN Thematic Guide to Night-time Light Remote Sensing and its Applications. pages 1–41. [5](#), [7](#)
- Elvidge, C. D., Erwin, E. H., Baugh, K. E., Ziskin, D., Tuttle, B. T., Ghosh, T., and Sutton, P. C. (2009). Overview of DMSp Nighttime Lights and Future Possibilities. [vii](#), [4](#), [6](#), [7](#), [9](#), [10](#), [11](#), [24](#)
- Elvidge, C. D., Imhoff, M. L., Baugh, K. E., Hobson, V. R., Nelson, I., and Dietz, J. B. (2000). Nighttime Lights of the World: 1994-95. [vii](#), [4](#), [6](#), [7](#), [9](#), [10](#), [11](#), [24](#)
- Ghosh, T., Anderson, S., Elvidge, C., and Sutton, P. ((2013)). Using Nighttime Satellite Imagery as a Proxy Measure of Human Well-Being. *Sustainability*, 5(12):4988–5019. [iii](#)
- Liu, Z., He, C., Zhang, Q., Huang, Q., and Yang, Y. (2012). Extracting the dynamics of urban expansion in China using DMSp-OLS nighttime light data from 1992 to 2008. *Landscape and Urban Planning*, 106(1):62–72. [5](#), [14](#)

- Ma, T., Zhou, C., Pei, T., Haynie, S., and Fan, J. ((2012)). Quantitative estimation of urbanization dynamics using time series of DMSP/OLS nighttime light data: A comparative case study from China's cities. *Remote Sensing of Environment*, 124:99–107. [26](#)
- Mennis, J. ((2003)). Generating Surface Models of Population Using Dasymetric Mapping*. 55(August 2002):31–42. [25](#)
- Small, C., Pozzi, F., and Elvidge, C. ((2005)). Spatial analysis of global urban extent from DMSP-OLS night lights. *Remote Sensing of Environment*, 96(3-4):277–291. [26](#)
- Wu, S.-s., Qiu, X., and Wang, L. ((2005)). Population Estimation Methods in GIS and Remote Sensing: A Review. *GIScience & Remote Sensing*, 42(1):80–96. [17](#), [26](#)
- Zeng, C., Zhou, Y., Wang, S., Yan, F., and Zhao, Q. ((2011)). Population spatialization in China based on night-time imagery and land use data. *International Journal of Remote Sensing*, 32(24):9599–9620. [2](#)
- Zhao, N., Zhou, Y., and Samson, E. L. (2015). Correcting Incompatible DN Values and Geometric Errors in Nighttime Lights Time-Series Images. 53(4):2039–2049. [4](#), [7](#), [8](#), [9](#), [24](#)

Appendix A

Movement schemata of geometric correction for Sicily

	F121999	F141999	F142000	F142001
None movement	0.96979067	0.98320351	0.98553325	1
Left 1pixel	0.97322247	0.96659492	0.94611103	0.96727
Left 2pixels	0.93358255	0.90990784	0.8697849	0.899378
Right 1pixel	0.91172142	0.9430612	0.96527818	0.967425
Right 2 pixels	0.82457468	0.86847856	0.904598	0.90058
Up 1 pixel	0.93130714	0.93956624	0.94679162	0.954064
Down 1pixel	0.92774296	0.9471144	0.94698933	0.955352
Up 2pixels	0.84188872	0.84726896	0.85921662	0.862695
Down 2pixels	0.84117426	0.86573313	0.86419065	0.868651
Right 1pixel - Up 1pixel	0.87539058	0.90031151	0.92567765	0.924941
Right 2pixels - Up 2pixels	0.72303223	0.75199474	0.7879444	0.784844
Left 1pixel - Down 1pixel	0.87481757	0.91122795	0.93002985	0.929096
Left 2pixels - Down 2pixels	0.8143498	0.80627253	0.77149719	0.794436
Left 1pixel - Up 1pixel	0.93547284	0.92535112	0.91119486	0.927224
Left 2pixels - Up 2pixels	0.89809386	0.87275089	0.83942284	0.864557
Right 1pixel - Down 1pixel	0.87481757	0.91122795	0.93002985	0.929096
Right 2pixels - Down 2pixels	0.72688882	0.77707426	0.80393194	0.796259
Left 2pixels - Up 1pixel	0.89809386	0.87275089	0.83942284	0.864557
Left 1pixel - Up 2pixels	0.84567267	0.83591618	0.82944982	0.841319
Left 2pixels - Down 1pixel	0.89416962	0.87745742	0.83806143	0.865581
Left 1pixel - Down 2pixels	0.84399118	0.85129996	0.83178217	0.845649
Right 2pixels - Down 1pixel	0.79419365	0.84256996	0.87511202	0.868496
Right 1pixel - Down 2pixels	0.79600346	0.83573949	0.85043012	0.847532
Right 2pixels - Up 1pixel	0.79254808	0.82904447	0.86642479	0.862518
Right 1pixel - Up 2pixels	0.79399222	0.8132263	0.83995726	0.838187

	F142002	F142003	F152000	F152001
None movement	0.969148	0.982461	0.958543	0.971626
Left 1pixel	0.950308	0.964644	0.961688	0.979599
Left 2pixels	0.892235	0.908419	0.926004	0.94747
Right 1pixel	0.931393	0.945529	0.905589	0.913924
Right 2 pixels	0.858666	0.875307	0.825027	0.830123
Up 1 pixel	0.968789	0.937187	0.968464	0.958136
Down 1pixel	0.892403	0.946705	0.879834	0.913209
Up 2pixels	0.909004	0.844135	0.922708	0.893783
Down 2pixels	0.781959	0.864552	0.771998	0.818651
Right 1pixel - Up 1pixel	0.929139	0.902094	0.913012	0.900081
Right 2pixels - Up 2pixels	0.802941	0.758184	0.791484	0.765437
Left 1pixel - Down 1pixel	0.860141	0.912826	0.834288	0.862093
Left 2pixels - Down 2pixels	0.731637	0.807156	0.753025	0.801643
Left 1pixel - Up 1pixel	0.951072	0.921133	0.972639	0.967471
Left 2pixels - Up 2pixels	0.892821	0.868626	0.936166	0.9365
Right 1pixel - Down 1pixel	0.860141	0.912826	0.834288	0.862093
Right 2pixels - Down 2pixels	0.703783	0.778648	0.677468	0.712794
Left 2pixels - Up 1pixel	0.892821	0.868626	0.936166	0.9365
Left 1pixel - Up 2pixels	0.893804	0.830701	0.927466	0.902991
Left 2pixels - Down 1pixel	0.825972	0.87787	0.852504	0.89115
Left 1pixel - Down 2pixels	0.770001	0.85059	0.775494	0.824528
Right 2pixels - Down 1pixel	0.796893	0.847394	0.764202	0.786772
Right 1pixel - Down 2pixels	0.755348	0.835346	0.734753	0.77598
Right 2pixels - Up 1pixel	0.854826	0.835936	0.829733	0.816833
Right 1pixel - Up 2pixels	0.871713	0.814373	0.869874	0.840802

	F152002	F152003	F152004	F152005
None movement	0.976459	0.967135	0.977547	0.96042
Left 1pixel	0.98062	0.962549	0.964534	0.969913
Left 2pixels	0.94338	0.919078	0.912278	0.940149
Right 1pixel	0.919778	0.919692	0.936297	0.90306
Right 2 pixels	0.835003	0.842513	0.862677	0.820575
Up 1 pixel	0.94363	0.966172	0.943086	0.951632
Down 1pixel	0.932827	0.899706	0.936462	0.903991
Up 2pixels	0.862098	0.912502	0.860131	0.895923
Down 2pixels	0.847462	0.800154	0.853367	0.813667
Right 1pixel - Up 1pixel	0.888157	0.917334	0.902494	0.893571
Right 2pixels - Up 2pixels	0.741662	0.794276	0.761357	0.766262
Left 1pixel - Down 1pixel	0.881565	0.858141	0.899498	0.853121
Left 2pixels - Down 2pixels	0.823008	0.768293	0.802898	0.797805
Left 1pixel - Up 1pixel	0.948932	0.962303	0.931843	0.962634
Left 2pixels - Up 2pixels	0.913978	0.918414	0.882339	0.933994
Right 1pixel - Down 1pixel	0.881565	0.858141	0.899498	0.853121
Right 2pixels - Down 2pixels	0.737001	0.708462	0.76413	0.708455
Left 2pixels - Up 1pixel	0.913978	0.918414	0.882339	0.933994
Left 1pixel - Up 2pixels	0.867568	0.909435	0.851073	0.907072
Left 2pixels - Down 1pixel	0.901881	0.857967	0.875708	0.884424
Left 1pixel - Down 2pixels	0.850851	0.797771	0.842882	0.819885
Right 2pixels - Down 1pixel	0.80368	0.789771	0.831984	0.778792
Right 1pixel - Down 2pixels	0.803717	0.76546	0.82203	0.771139
Right 2pixels - Up 1pixel	0.806343	0.839001	0.831184	0.811177
Right 1pixel - Up 2pixels	0.813266	0.866825	0.824032	0.842032

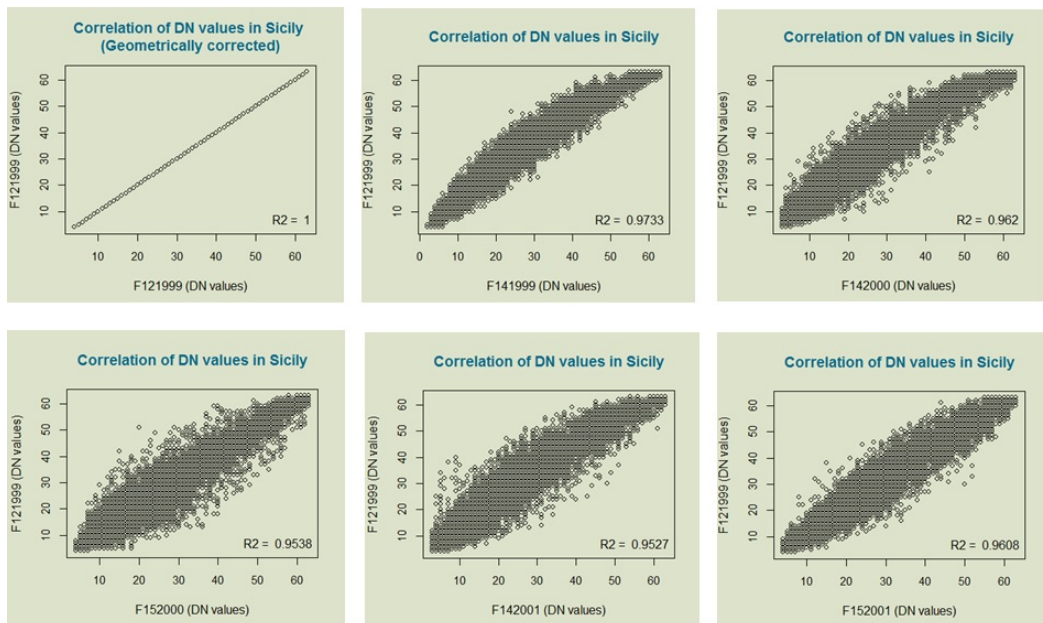
	F152006	F152007	F162004	F162005
None movement	0.976399	0.976143	0.953185	0.978883
Left 1pixel	0.961258	0.93669	0.951403	0.964946
Left 2pixels	0.909357	0.863328	0.91308	0.914501
Right 1pixel	0.939969	0.960975	0.907282	0.942583
Right 2 pixels	0.872612	0.908281	0.833921	0.875308
Up 1 pixel	0.95616	0.938608	0.964302	0.930664
Down 1pixel	0.924983	0.938369	0.872434	0.954017
Up 2pixels	0.88798	0.854297	0.9196	0.839055
Down 2pixels	0.835738	0.85674	0.762811	0.8841
Right 1pixel - Up 1pixel	0.920105	0.922387	0.917167	0.896149
Right 2pixels - Up 2pixels	0.796899	0.793655	0.805873	0.755408
Left 1pixel - Down 1pixel	0.892489	0.925663	0.832259	0.920263
Left 2pixels - Down 2pixels	0.786435	0.767142	0.740606	0.830932
Left 1pixel - Up 1pixel	0.942129	0.902914	0.962472	0.918043
Left 2pixels - Up 2pixels	0.891508	0.834243	0.922736	0.871016
Right 1pixel - Down 1pixel	0.892489	0.925663	0.832259	0.920263
Right 2pixels - Down 2pixels	0.756048	0.805561	0.67634	0.798834
Left 2pixels - Up 1pixel	0.891508	0.834243	0.922736	0.871016
Left 1pixel - Up 2pixels	0.875772	0.824892	0.91768	0.828377
Left 2pixels - Down 1pixel	0.864405	0.83259	0.839962	0.892583
Left 1pixel - Down 2pixels	0.824542	0.824819	0.763959	0.872249
Right 2pixels - Down 1pixel	0.83119	0.877748	0.767884	0.856846
Right 1pixel - Down 2pixels	0.808227	0.846326	0.729346	0.854649
Right 2pixels - Up 1pixel	0.854159	0.870935	0.842177	0.832772
Right 1pixel - Up 2pixels	0.855689	0.839039	0.875596	0.809619

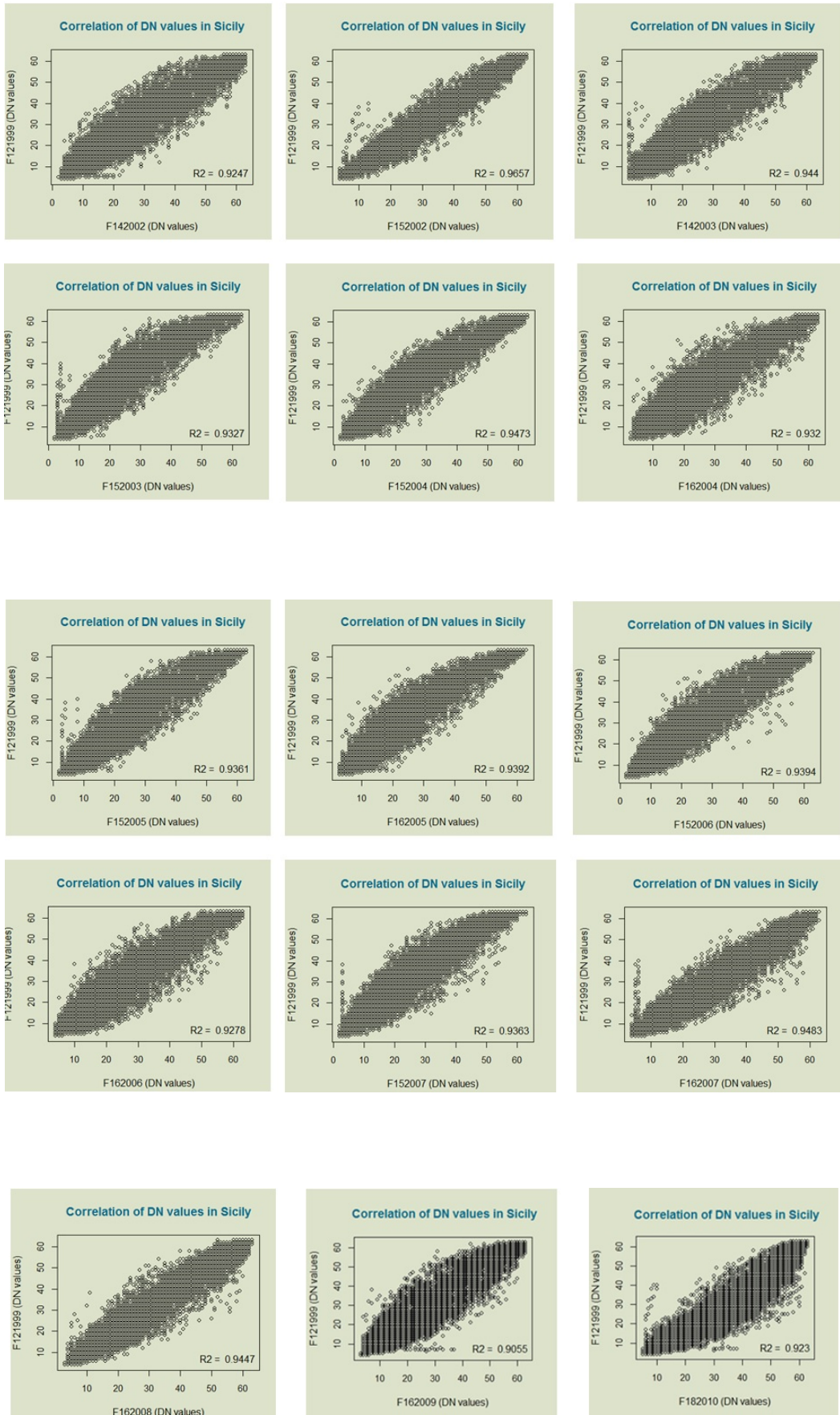
	F162006	F162007	F162008	F162009
None movement	0.976195	0.972465	0.962777	0.892233
Left 1pixel	0.950726	0.969986	0.969724	0.879949
Left 2pixels	0.891052	0.930036	0.939464	0.838765
Right 1pixel	0.951042	0.926287	0.909857	0.864214
Right 2 pixels	0.893365	0.852061	0.831917	0.810075
Up 1 pixel	0.930863	0.931967	0.934612	0.956757
Down 1pixel	0.947632	0.936556	0.918459	0.794117
Up 2pixels	0.842356	0.846034	0.859089	0.954336
Down 2pixels	0.874157	0.856637	0.834995	0.677079
Right 1pixel - Up 1pixel	0.907903	0.888542	0.884753	0.927415
Right 2pixels - Up 2pixels	0.778815	0.749275	0.752509	0.868353
Left 1pixel - Down 1pixel	0.923458	0.893291	0.868878	0.768567
Left 2pixels - Down 2pixels	0.808786	0.827035	0.824973	0.655649
Left 1pixel - Up 1pixel	0.906377	0.929366	0.939826	0.939603
Left 2pixels - Up 2pixels	0.849731	0.891116	0.908895	0.889871
Right 1pixel - Down 1pixel	0.923458	0.893291	0.868878	0.768567
Right 2pixels - Down 2pixels	0.803172	0.757599	0.727848	0.616667
Left 2pixels - Up 1pixel	0.849731	0.891116	0.908895	0.889871
Left 1pixel - Up 2pixels	0.820427	0.843226	0.862106	0.934616
Left 2pixels - Down 1pixel	0.86939	0.898837	0.901109	0.756315
Left 1pixel - Down 2pixels	0.855378	0.856307	0.844017	0.67543
Right 2pixels - Down 1pixel	0.868344	0.823588	0.796201	0.721944
Right 1pixel - Down 2pixels	0.852178	0.818601	0.791183	0.654786
Right 2pixels - Up 1pixel	0.854252	0.818526	0.810573	0.86823
Right 1pixel - Up 2pixels	0.823918	0.809106	0.816754	0.926631

	F182010
None movement	0.902607
Left 1pixel	0.862801
Left 2pixels	0.799447
Right 1pixel	0.901812
Right 2 pixels	0.870102
Up 1 pixel	0.956336
Down 1pixel	0.813251
Up 2pixels	0.942801
Down 2pixels	0.703817
Right 1pixel - Up 1pixel	0.955144
Right 2pixels - Up 2pixels	0.904796
Left 1pixel - Down 1pixel	0.812209
Left 2pixels - Down 2pixels	0.644228
Left 1pixel - Up 1pixel	0.911644
Left 2pixels - Up 2pixels	0.840098
Right 1pixel - Down 1pixel	0.812209
Right 2pixels - Down 2pixels	0.67931
Left 2pixels - Up 1pixel	0.840098
Left 1pixel - Up 2pixels	0.898789
Left 2pixels - Down 1pixel	0.729884
Left 1pixel - Down 2pixels	0.681522
Right 2pixels - Down 1pixel	0.785419
Right 1pixel - Down 2pixels	0.701431
Right 2pixels - Up 1pixel	0.919303
Right 1pixel - Up 2pixels	0.94097

Appendix B

Intercalibration scattergrams (Geometrically corrected Sicily)





Appendix C

Testing data normality

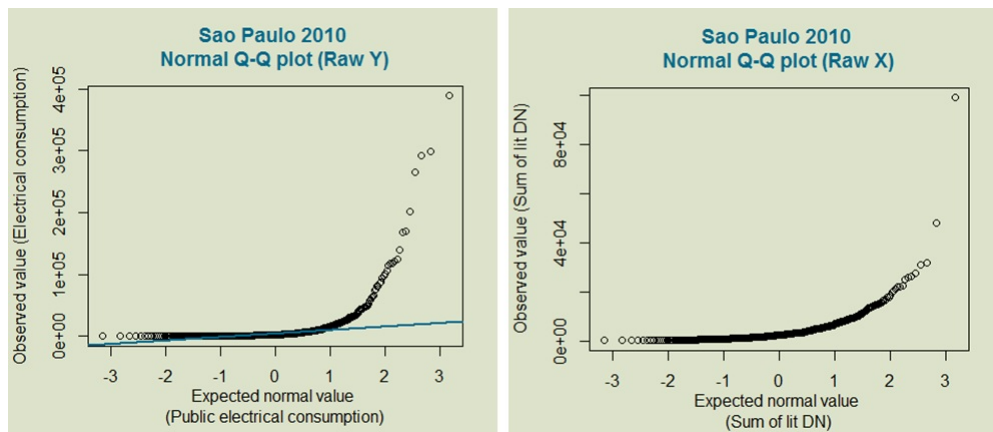


Figure C.1: Quantile-Quantile plot: (a) Raw Y and (b) Raw X.

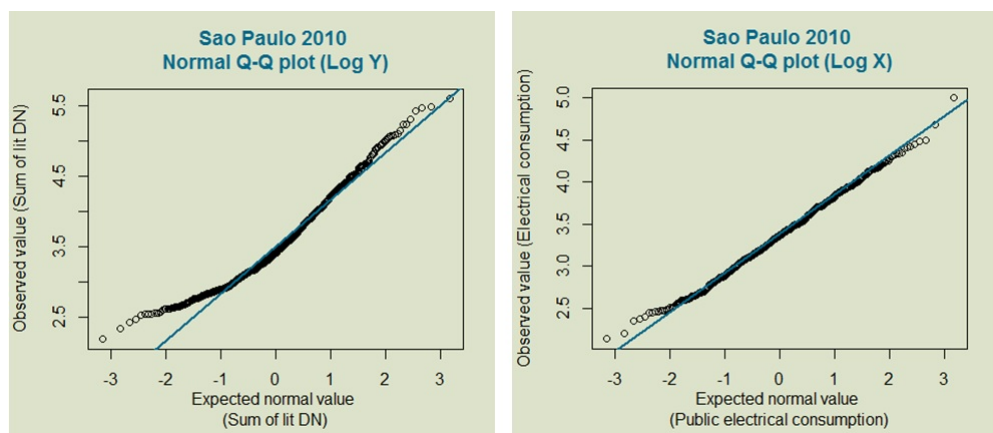


Figure C.2: Quantile-Quantile plot: (a) Log Y and (b) Log X.

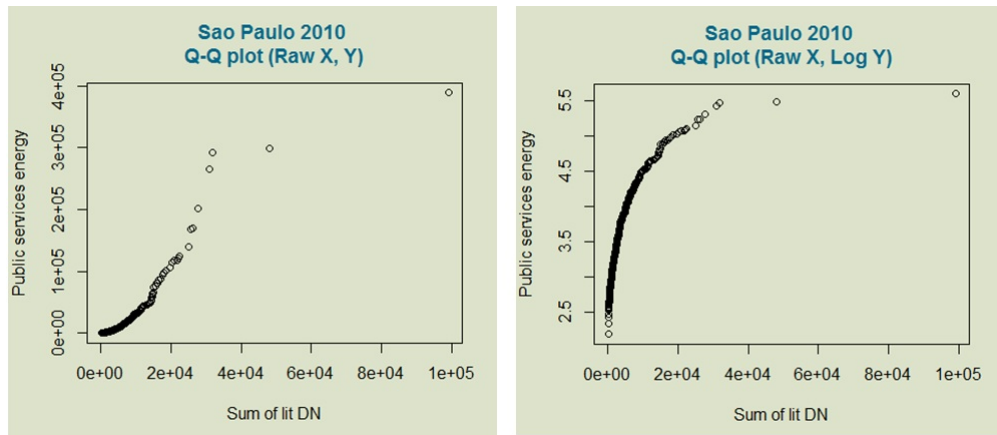


Figure C.3: Quantile-Quantile plot: (a) Raw X, Log Y and (b) Log X, Row Y.

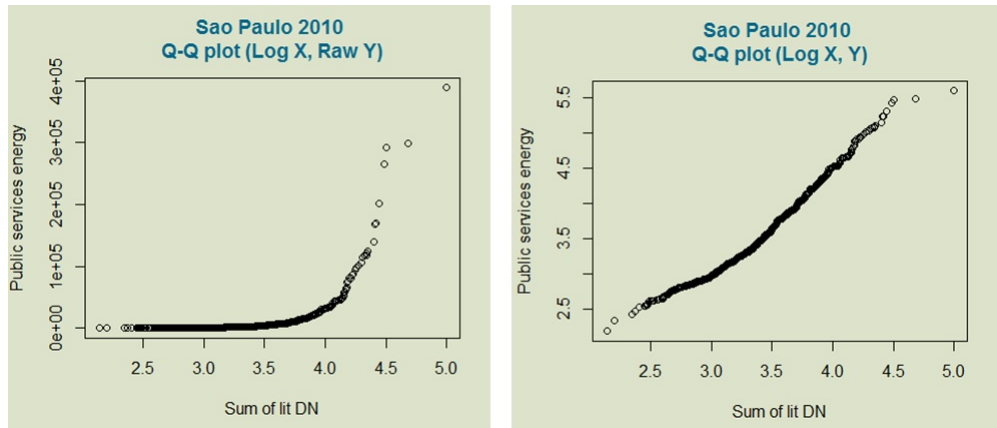


Figure C.4: Quantile-Quantile plot: (a) Log X, Raw Y and (b) Raw X, Log Y.

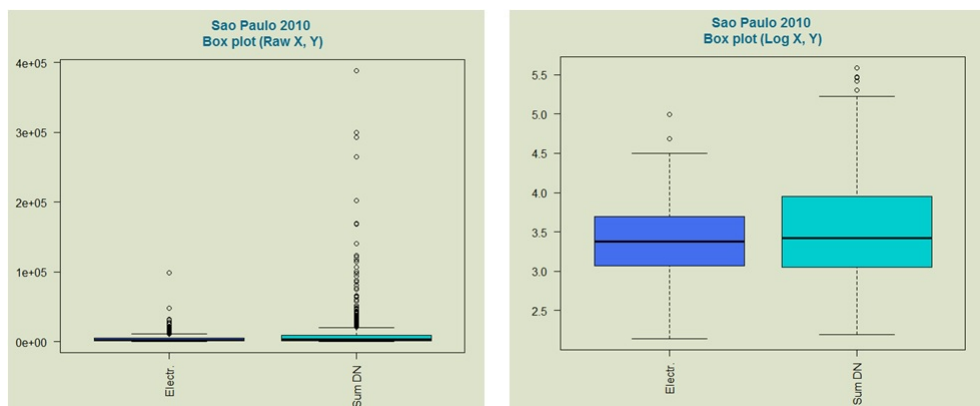


Figure C.5: Box plot: (a) Before log-transformation (b) After log-transformation of X and Y axes.

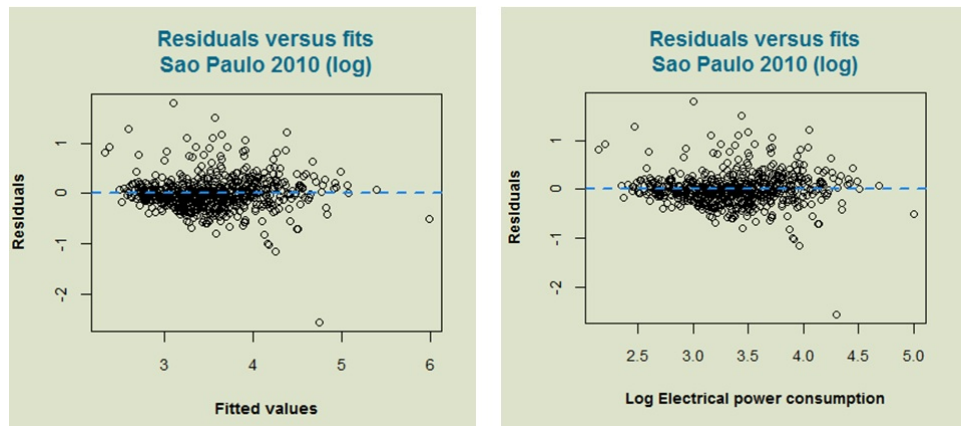


Figure C.6: Residuals: (a) Against fitted values (b) Against logarithmic electric power consumption data.

Appendix D

Frequency analysis and standardisation of values

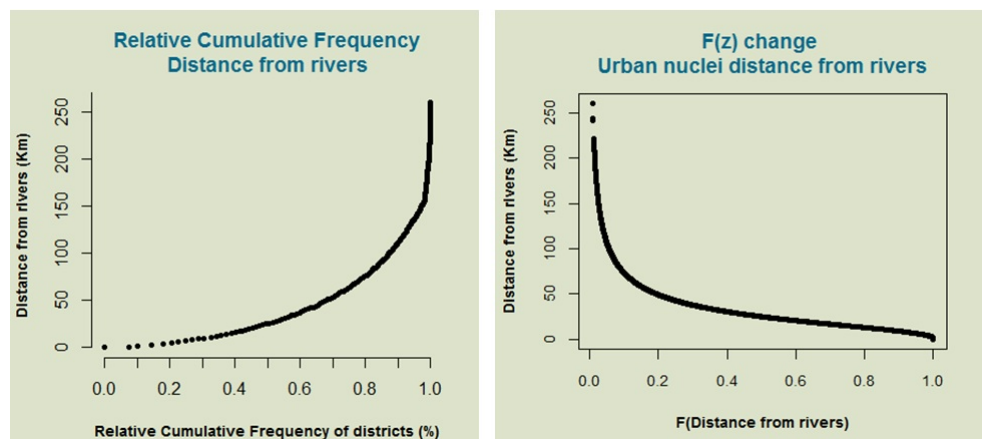


Figure D.1: Urban nuclei distance from rivers (a) Accumulated frequency and (b) Standardized values.

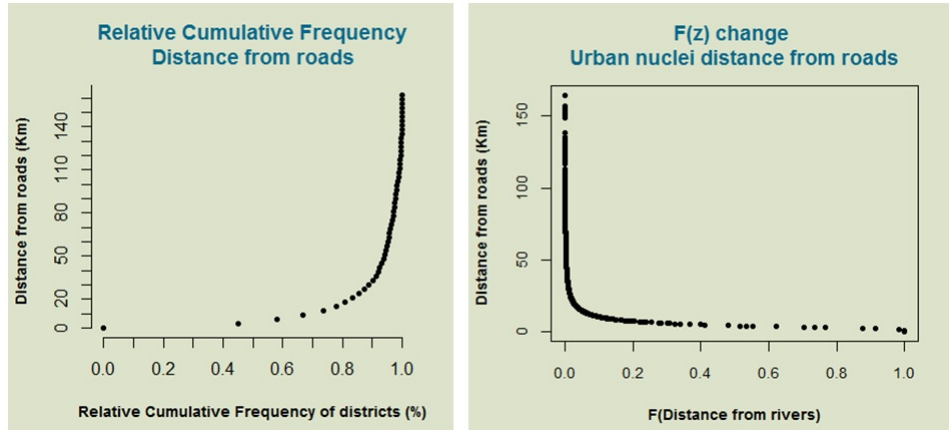


Figure D.2: Urban nuclei distance from road network (a) Accumulated frequency and (b) Standardized values.

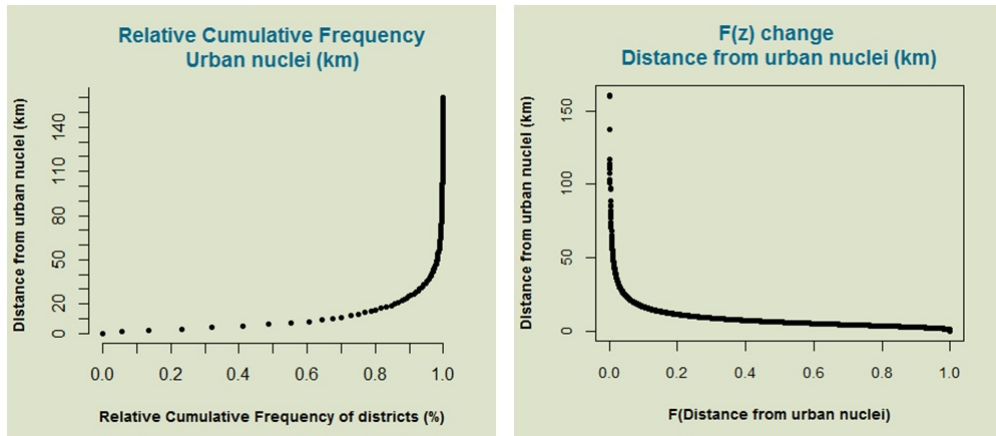


Figure D.3: Urban nuclei distance from nearest neighbour (a) Accumulated frequency and (b) Standardized values.

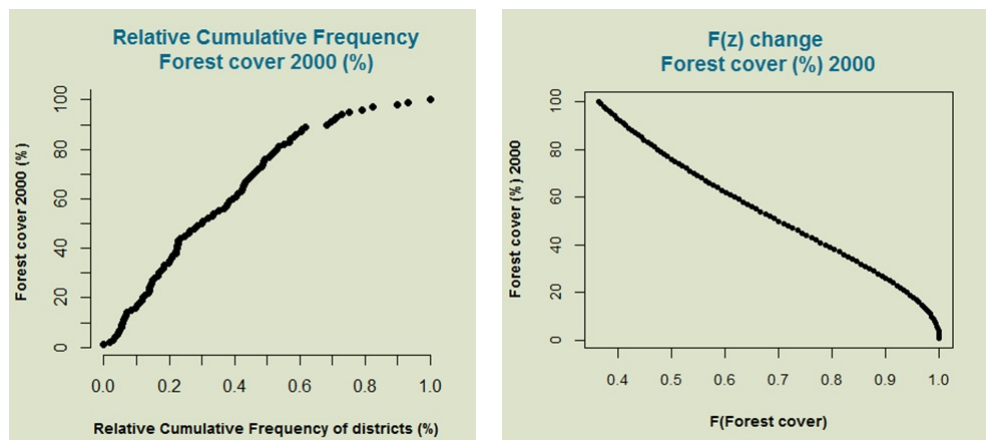


Figure D.4: Urban nuclei and forest cover 2000 (a) Accumulated frequency and (b) Standardized values.

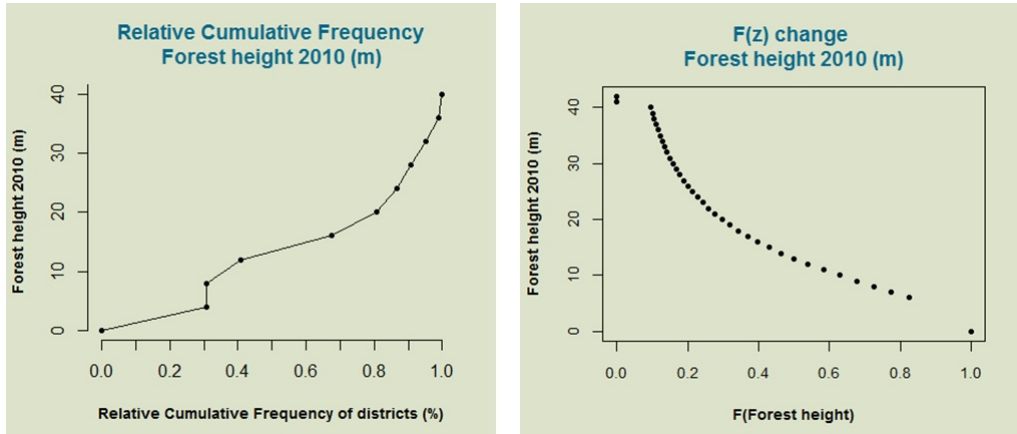


Figure D.5: Urban nuclei and forest height 2010 (a) Accumulated frequency and (b) Standardized values.

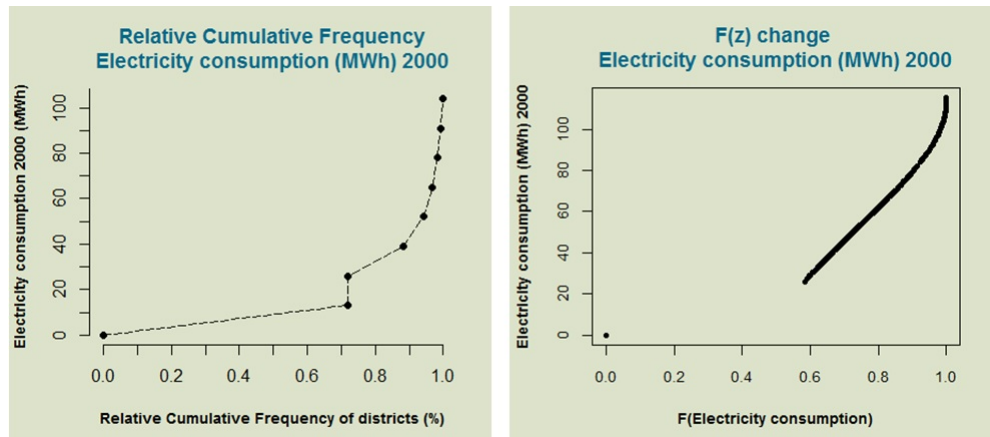


Figure D.6: Urban nuclei and electric power consumption 2000 (a) Accumulated frequency and (b) Standardized values.

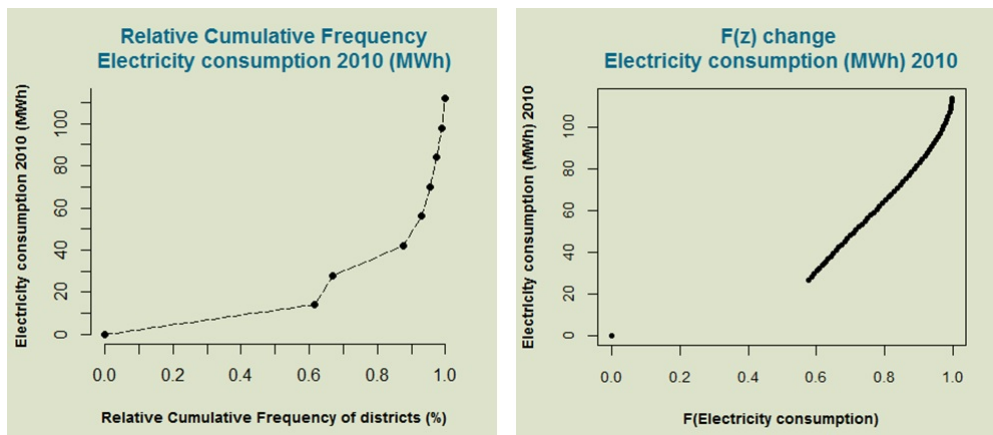


Figure D.7: Urban nuclei and electric power consumption 2010 (a) Accumulated frequency and (b) Standardized values.